

Running head: DYNAMIC MODEL OF DECISION-MAKING

Indiana University Cognitive Science Tech Report #232

Multi-Alternative Decision Field Theory:

A Dynamic Artificial Neural Network Model of Decision-Making

Robert M. Roe, Jerome R. Busemeyer, and James T. Townsend

Indiana University

June 22, 1999

Please address all correspondence to:

Robert M. Roe
Department of Psychology
Indiana University
1101 E. 10th Street
Bloomington IN, 47405-7007
Email: rmroe@indiana.edu
Phone: 812-856-4678
Fax: 812-855-4691

Abstract

Decision field theory (Busemeyer & Townsend, 1993) is interpreted as an artificial neural network and extended to accommodate multi-alternative preferential choice situations. The classic weighted additive utility model and the classic Thurstone preferential choice model are shown to be special cases of the new theory, and the proposed theory also can emulate the search process of the popular elimination by aspects model. The new theory explains several central empirical results found in the multi-alternative preference literature, including the similarity effect, the attraction effect, and the compromise effect. Furthermore, it is the only formal theory that has succeeded in explaining the complex interactions among these three effects. The dynamic nature of the model also allows strong testable predictions as to the effect of time pressure on these three effects.

Introduction

Preferential choice is a complex topic that requires examination from many different perspectives. Take, for example, the relatively simple task of buying a new car. From one point of view, this is a search problem in which a very large set of options is winnowed down to a much smaller set of satisfactory options (Simon, 1955; Tversky, 1972). From another point of view, this is an evaluation problem requiring tradeoffs among multiple conflicting attributes such as safety, quality, performance, and cost (Keeney & Raiffa, 1976; Von Winterfeldt & Edwards, 1986). From a third point of view, this is a preferential choice problem in which the candidates engage in a competition, and the winning alternative is probabilistically chosen (De Soete, Feger, & Klauer, 1989; Thurstone, 1959).

The major goal of this article is to present a general decision theory that encompasses all of these points of view within a single theoretical framework. Initial but critical probing of the theory's ability to predict several central findings in multi-alternative choice is offered. The present theory is an elaboration of an earlier theory known as decision field theory, which was originally developed to explain choice behavior for decision-making under uncertainty by Busemeyer & Townsend (1993). Later, Townsend & Busemeyer (1995) extended it to explain the relation between choice, selling prices, and certainty equivalents. More recently, it was extended to account for multi-attribute decision making by Diederich (1997). However, all of these previous developments were limited to choice situations involving only two choice options. This simplification was initially necessary to focus on other issues in more depth such as multi-attribute outcomes and multiple uncertain outcomes. The present development

relaxes this restriction and presents an extension of decision field theory to multiple (more than two) preferential choice problems. Many new and complex issues arise with multi-alternative choice problems that do not appear in the simpler binary choice task -- for example, a winnowing search process is unnecessary in the binary choice task, but it becomes crucial when choosing from a large set of alternatives.

A very large literature already exists on the topic of preferential choice with multiple options (see Mellers, Schwartz, & Cooke, 1998; Payne, Bettman, & Johnson, 1992, for reviews). What is unique about decision field theory is that it describes the dynamic process that ensues between the onset of the choice task and the final selection. This dynamic formulation permits the theory to explain the systematic relations between choice probability and decision time, and the important effects of time pressure on choice probability.

A second purpose of this article is to build formal connections between decision field theory and other artificial neural network models of decision processes (e.g. Grossberg & Gutowski, 1987, Usher & Zakay, 1993, & Levin & Levine, 1996). Decision field theory is recast in terms of an artificial neural network, and the principle of *lateral inhibition* (cf. Grossberg, 1988) is incorporated into the theory. Lateral inhibitory connections between response nodes turns out to play a critical role in explaining paradoxical findings from the preferential choice literature.

The remainder of this article is organized as follows. First we introduce the basic ideas of Multi-alternative Decision Field Theory (MDFT). In this first section, we also show how the classic multi-attribute value model (Von Winterfeldt & Edwards, 1986) and the classic preferential choice model (Thurstone, 1959; De Soete et al., 1989) can be

derived as special cases from MDFT under certain ideal conditions and task constraints. Second, we review the central or pivotal empirical findings from research on multiple alternative choice. This includes (a) the similarity effect produced by adding a similar competing alternative to the choice set, (b) the attraction effect produced by adding a dominated alternative to the choice set, (c) the compromise effect produced by adding a intermediate alternative to the choice set, and (d) the effects of time pressure on preferential choice. The similarity effect is important because it produces violations of general property called *independence from irrelevant alternatives*, and the attraction effect is important because it violates another general property called *regularity*. Third, we show how the winnowing search process of the elimination-by-aspects model (Tversky, 1972) can be mimicked by alternative versions of MDFT. Although specific alternative explanations have been proffered for each of these central qualitative findings, this is the first attempt to account for all of these effects within a single theory. Finally, we compare the explanatory power of MDFT with other preferential choice models

Multiple Choice Decision Field Theory

A simple example is presented to make the description of the theory more concrete. Consider the case of a new car purchase where the choice set has been reduced to three cars, which differ primarily on only two attributes, performance quality and gas mileage. Note that this example is solely for illustrative purposes, and the theory is more generally applicable. The formal model can accommodate an arbitrary number of attributes and alternatives.

The basic intuition underlying decision field theory is that decision maker's preferences for each option evolve during deliberation by integrating a stream of

comparisons among options on evaluations of attributes over time. Initially, the decision-maker's attention may focus on the most important attribute (e.g., performance) and some specific aspects (e.g., acceleration, control on turns, stability at high speeds) of this attribute are evaluated for a period of time. During this time period, the evaluation of each option is compared to others, and these comparisons change the preferences up or down depending on whether or not an option has an advantage or disadvantage on the attended attribute. A few moments later, attention may switch to another less important attribute (gas mileage), and comparisons of specific aspects (e.g., rising gas prices, environmental concerns) related to this second attribute are added to the previous preferences. Attention may then switch back to an earlier attribute for additional comparisons, and these comparisons continue to update the preferences for each option. Eventually a decision is reached either by an externally imposed time constraint (e.g., the car dealer presses for a final decision), or by a self imposed criterion (e.g., preference exceeds a threshold and the buyer announces a decision). According to this interpretation, decision field theory falls within the class of preferential choice models known as sequential sampling models (cf., Aschenbrenner, Albert, & Schmalhofer, 1984).

Artificial Neural Network Interpretation.

The artificial neural networks shown in Figures 1 and 2 are used to represent the intuitions described above. The theory is composed of two stages – the first stage computes a quantity called the valence input (a network interpretation of Lewin's , 1935, original concept) for each alternative at each moment, and the second stage computes a quantity called the preference state (a dynamic interpretation of the classic decision theoretic concept) for each alternative at each moment.

The connectionistic feed-forward network (c.f. Rumelhart & McClelland, 1986) shown in Figure 1 illustrates the first stage. The evaluation nodes (labeled **M**) at the top of the figure represent the evaluations of each alternative on each attribute. For example, if the decision is to choose among three cars on the basis of quality and gas mileage attributes, then there are six possible evaluations. (Of course, a real car purchase entails many more attributes and alternatives). These evaluations are filtered by momentary attention weights (labeled **W**) linked to the attributes. Subsequently, the weighted evaluations are transformed by contrast weights (labeled **C**) to produce comparisons among the weighted evaluations. The final outputs (labeled **V**) in Figure 1 are the valences, which represent the advantage or disadvantage being considered for each alternative at a particular time point. These valences change stochastically over time as the decision-maker's attention shifts unpredictably from one attribute to another.

<Insert Figure 1 about here>

The competitive recursive network (c.f., Grossberg, 1988) shown in Figure 2 illustrates the second stage. The three nodes (labeled A, B, and C) represent the three choice alternatives (e.g., three cars). More generally, there is one decision node in the recursive network corresponding to each choice alternative.

The input into each decision node is the valence previously described in Figure 1. The output activation from each node represents the strength of preference for the corresponding alternative at a particular point in time. The activation level increases with positive valences (advantages) and decreases with negative valences (disadvantages). Thus the activation of a node at any point in time represents the evolving preference formed by the temporal integration of the stream of input valences.

Each node in the network is connected with every other node and each node also has a self-feedback loop. The self-feedback loop allows activation within a node to grow or decay over time. This is needed to integrate the valences for a given option over time. If the strength of a self-feedback loop is set to zero, then that node would have no memory of its previous state of activation. If the strength of the self-connection is set to one, then that node has perfect memory of its previous state of activation. Intermediate strengths, between zero and one, provide partial memory and limited decay.

The interconnections among nodes represent a competitive system so that activation of one node inhibits the other nodes. The strength of the negative interconnection between a pair of nodes determines the strength of inhibition passed from one node to another. The interconnection strengths are assumed to depend on the perceived similarity between alternatives within the attribute space used to characterize the options. These similarity relations will become clearer when we analyze specific cases later in this article. The general principle is that the interconnection strength is a decreasing function of the psychological distance between options. Highly similar options compete with each other more than highly dissimilar options. This corresponds to the principle of lateral inhibition used in competitive networks (cg. Grossberg, 1988). Lateral inhibition is a key principle for producing enhancement effects for the strongest alternative within a cluster of highly similar alternatives.

<Insert Figure 2 about here>

Multivariate Dynamic Stochastic System.

The artificial neural network illustrated in Figures 1 and 2 provides a useful framework for interpreting MDFT. However, the explanatory power of the theory derives

from a more formal representation in terms of a multivariate dynamical system described next. (Readers not interested in these formalities can skip to the application sections).

The input valence for each option, $v_i(t)$, represents one of the coordinates of a valence vector, $\mathbf{V}(t)$ at time t . The output preference for each option, $P_i(t)$, represents one of the coordinates of a preference state vector, $\mathbf{P}(t)$ at time t . The self-connections and interconnections form a feedback matrix \mathbf{S} , with element S_{ij} representing the connection between nodes i and j . Based on these definitions, the preference state changes from $\mathbf{P}(t)$ at time t to $\mathbf{P}(t+1)$ a small moment later at time $(t+1)$ according to the following linear stochastic difference equation:

$$\mathbf{P}(t+1) = \mathbf{S} \mathbf{P}(t) + \mathbf{V}(t+1) \quad (1)$$

Thus the new state of preference is a linear transformation of the previous state plus the new input valence. The dynamic behavior of this model is determined by three factors: The initial preference state $\mathbf{P}(0)$ at the beginning of the choice (time $t = 0$), the new input valence $\mathbf{V}(t)$, and the feedback matrix \mathbf{S} .

Initial Preference State. In general, the initial preference state represents a residual bias left over from previous experience with choice problems. For example, status quo effects (Samuelson & Zeckhauser, 1989), previous habits, or experience and memory for the previous history of choices can be captured by the initial state. For novel choice problems, the initial state may be considered unbiased, in which case $\mathbf{P}(0)=\mathbf{0}$. The applications presented below are based on the latter assumption.

Input Valence. The input valence represents comparisons among alternatives on evaluations of attributes. These comparisons vary from moment to moment due to

changes and fluctuations in attention to the attributes over time. As illustrated in Figure 1, the input valence is computed from three different components \mathbf{M} , \mathbf{W} , and \mathbf{C} .

The first component is the evaluation matrix \mathbf{M} , which represents all of the possible evaluations of the alternatives on the attributes. As a simple example, the car decision problem has two primary attributes -- gas mileage and performance quality. Define $\mathbf{G} = [g_A, g_B, g_C]'$ as a vector of evaluations for the three cars on gas mileage. For example, if car A gets lower gas mileage than car C, then g_A is assigned a lower scale value than g_C , so that $g_A < g_C$. Similarly, define $\mathbf{Q} = [q_A, q_B, q_C]'$ as a vector of evaluations for the three cars on performance quality. For example if car A has higher quality than car C, then q_A is assigned a higher scale value than q_C , so that $q_A > q_C$. Concatenation of these two evaluation vectors forms a 3×2 value matrix, denoted $\mathbf{M} = [\mathbf{G} | \mathbf{Q}]$.

The second component is the attention weight vector, $\mathbf{W}(t)$. The momentary attention to attribute j is represented by an attention weight, $w_j(t)$, at time t . In the simple car purchase example, there are two attention weights, $w_g(t)$ for gas mileage, and $w_q(t)$ for performance quality. The attention weights for all the aspects of the attributes form a weight vector $\mathbf{W}(t) = [w_g(t) \ w_q(t)]'$.

The product of weights and values, $\mathbf{MW}(t)$, determines the weighted value of each alternative at each time point. This product can be viewed as a stochastic version of the classic multi-attribute weighted additive value model. For example, when choosing among three cars, the i -th row of the product $\mathbf{MW}(t)$ equals $w_g(t) g_i + w_q(t) q_i$, which is stochastic due to fluctuations in the attention weights $w_g(t)$ and $w_q(t)$.

The third component is the contrast matrix, C , which is used to represent the comparisons among alternatives. In general, the contrast for each alternative is defined by comparing the weighted value of one alternative to the average of all the others. More specifically, in the case of two and three alternatives, the contrast matrix becomes

$$C = \begin{bmatrix} 1/2 & -1/2 \\ -1/2 & 1/2 \end{bmatrix} \quad C = \begin{bmatrix} 1 & -1/2 & -1/2 \\ -1/2 & 1 & -1/2 \\ -1/2 & -1/2 & 1 \end{bmatrix}$$

Based on these three definitions, the valence vector is formed by the product

$$V(t) = C M W(t). \quad (2a)$$

The car purchase example described above contained only three alternatives described by two primary attributes for simplicity. However, most decisions usually involve a larger number of attributes, and Equation 2a is applicable with arbitrary numbers of alternatives and attributes. But in practice, it is useful to group the possibly large number of attributes into two subgroups, a relatively small subgroup of primary attributes of importance, and a larger subgroup of irrelevant attributes. For example, the experiments discussed later usually design the options by manipulating a few primary dimensions, but these options may also differ on a number of other irrelevant attributes. Even in these more complex settings, a simplified analysis can be performed by partitioning a p -dimensional attention weight vector into two components $W(t)' = [W_1(t)', W_2(t)']$, where $W_1(t)$ is a q -dimensional component containing the primary dimensions and $W_2(t)$ contains the remaining $p-q$ irrelevant dimensions. Then Equation 2a can be rewritten in terms of the primary and irrelevant dimensions as follows:

$$\mathbf{V}(t) = \mathbf{C} \mathbf{M} \mathbf{W}(t) = \mathbf{C} \mathbf{M}_1 \mathbf{W}_1(t) + \boldsymbol{\varepsilon}(t), \quad (2b)$$

where $\boldsymbol{\varepsilon}(t) = \mathbf{C} \mathbf{M}_2 \mathbf{W}_2(t)$ can be treated as an stochastic error or residual term.

The valence vector defined by Equation 2a is a linear transformation of the stochastic weight vector, $\mathbf{W}(t)$. This weight vector is assumed to change across time according to a stationary stochastic process. For example, in the applications presented below, attention is assumed to switch back and forth from one attribute to another according to a simple Bernoulli process.¹ The stationarity assumption for the weights implies that the valence vector is also a stationary stochastic process with mean

$$\begin{aligned} E[\mathbf{V}(t)] &= E[\mathbf{C} \mathbf{M}_1 \mathbf{W}_1(t) + \boldsymbol{\varepsilon}(t)] \\ &= \mathbf{C} \mathbf{M}_1 E[\mathbf{W}_1(t)] + E[\boldsymbol{\varepsilon}(t)] = \mathbf{C} \mathbf{M}_1 \mathbf{W}_1 + \mathbf{0} = \boldsymbol{\mu}, \end{aligned}$$

and variance - covariance matrix at each time point given by

$$\begin{aligned} Cov[\mathbf{V}(t)] &= Cov[\mathbf{C} \mathbf{M}_1 \mathbf{W}_1(t) + \boldsymbol{\varepsilon}(t)] \\ &= \mathbf{C} \mathbf{M}_1 Cov[\mathbf{W}_1(t)] \mathbf{M}_1' \mathbf{C}' + Cov[\boldsymbol{\varepsilon}(t)] \\ &= \mathbf{C} \mathbf{M}_1 \boldsymbol{\Psi} \mathbf{M}_1' \mathbf{C}' + \boldsymbol{\zeta} = \boldsymbol{\Phi} \end{aligned}$$

where $\boldsymbol{\Psi} = Cov[\mathbf{W}_1(t)] = E[(\mathbf{W}_1(t) - \mathbf{W}_1)(\mathbf{W}_1(t) - \mathbf{W}_1)']$ is the variance – covariance matrix for the primary weights, and $\boldsymbol{\zeta} = Cov[\boldsymbol{\varepsilon}(t)] = E[\boldsymbol{\varepsilon}(t)\boldsymbol{\varepsilon}(t)']$ is the variance – covariance matrix of the residuals. Analogous to a factor analytic model (cf., Takane., 1989), the residuals are assumed to be uncorrelated with the primary dimensions and uncorrelated with each other. This implies that $\boldsymbol{\zeta}$ is a diagonal matrix.

Feedback Matrix. The feedback matrix, \mathbf{S} , is a full rank matrix containing the self-connections and interconnections among the choice nodes. The interconnection, S_{ij} for $i \neq j$, is a decreasing function of the psychological distance between options i and j . The psychological distance between alternatives is based on their positions in the multi-

attribute evaluation space. In other words, each alternative is represented as a point in a multidimensional space with dimensions defined by the attributes used to characterize the choice alternatives. For example, Figure 5 shown later in this article illustrates a small set of cars placed within a two dimensional space characterized by performance quality and gas mileage. Car A is high on performance and low on gas mileage, whereas car B is low on performance and high on gas mileage. In this example, options A and B are highly dissimilar, and another option, C2, is highly similar to option A. Thus options A and C2 have stronger inhibitory interconnections than options A and B or C2 and B. More details about the way the psychological distance between options affects the interconnections between nodes is provided later when we examine specific experimental conditions.

The effects of the feedback matrix on the evolution of preference over time can be seen more clearly by expanding Equation 1 :

$$\mathbf{P}(t) = \sum_{j=0, t-1} \mathbf{S}^j \mathbf{V}(t-j) + \mathbf{S}^t \mathbf{P}(0). \quad (3)$$

This equation shows that the current preference state can be viewed as a weighted sum of the previous input valences. The weight placed on each previous input is determined by the feedback matrix raised to a power, where the power equals the lag between the current state and the previous input. For this system to be stable, the eigenvalues of the feedback matrix must be less than one in magnitude. In this case, the effect of the feedback matrix decays toward zero as the lag increases in value. Taking expectations and simplifying produces the mean preference over time:

$$\xi(t) = E[\mathbf{P}(t)] = (\mathbf{I} - \mathbf{S})^{-1}(\mathbf{I} - \mathbf{S}^t) \boldsymbol{\mu} + \mathbf{S}^t \mathbf{P}(0). \quad (4)$$

For stable systems, as $t \rightarrow \infty$, then $\xi(t) \rightarrow (\mathbf{I} - \mathbf{S})^{-1} \mu$, which is a simple formula for analyzing the effects of the feedback matrix on the asymptotic mean preference state.

If weights are identically and independently distributed over time (see Footnote 1), then the variance – covariance matrix of the preference state evolves over time according to:

$$\begin{aligned} \Omega(t) &= \text{Cov}[\mathbf{P}(t)] = E \{ (\mathbf{P}(t) - E[\mathbf{P}(t)]) (\mathbf{P}(t) - E[\mathbf{P}(t)])' \} \\ &= \sum_{j=0, t-1} \mathbf{S}^j \Phi \mathbf{S}^{j'} \end{aligned} \quad (5)$$

Multi-Attribute Utility Model. If the feedback matrix is set to zero ($\mathbf{S}=\mathbf{0}$), then according to Equation 1, the preference state equals the valence input, $\mathbf{P}(t)=\mathbf{V}(t)$. If it is also assumed that attention does not fluctuate across time ($\Psi=\mathbf{0}$) and the residual variances are zero ($\zeta=\mathbf{0}$), then valence $\mathbf{V} = \mathbf{CMW}$ reduces exactly to differences between classic multi-attribute weighted additive values (cf. Von Winterfeldt & Edwards, 1986). Applying the car purchase example to this special case, the valence for say option A reduces to

$$v_A = (w_g g_A + w_q q_A) - [(w_g g_B + w_q q_B) + (w_g g_C + w_q q_C)]/2.$$

Furthermore, $v_A > \text{Max}(v_B, v_C)$ implies that $(w_g g_A + w_q q_A) > \text{Max}[(w_g g_B + w_q q_B), (w_g g_C + w_q q_C)]$. Thus, \mathbf{V} produces exactly the same rank order over alternatives as the classic multi-attribute model under these restrictive conditions.

Externally Controlled Stopping Time

Eventually, the evolving output preferences, $\mathbf{P}(t)$, determine the final choice. But the specific decision rule for determining this choice varies depending on whether the decision time is externally imposed versus subject controlled, as described next.

Choice tasks are termed externally controlled when the decision is made at an appointed time or designated time point (cf. Ratcliff, 1978; Vickers, Burt, Smith &

Brown, 1985). For example, a woman who has just received a proposal for marriage may be asked to announce her decision the next morning. As another example, a young man who has just been offered a job may be asked to sign his contract by the end of the week. For the car choice example, the car dealer, upon seeing other customers waiting for help, may lose his patience, interrupt the purchaser, and pressure him or her to make an immediate decision.

Figure 3 represents this type of choice task for the new car example. The abscissa represents time while the ordinate represents the level of preference of each option. The three trajectories labeled A, B, and C represent the preferences of each option as they evolve stochastically over time according to Equation 1. The vertical line to the right represents the appointed time for the decision. In this case, the option with the highest preference at the designated time point is the one chosen (option C in the Figure).

<Insert Figure 3 about here>

As can be seen in the above figure, the fact that preferences cross over time implies that different choices may result depending on the designated time to make the decision. For example, if the appointed time was shortened to time t_1 shown in the figure, then alternative B would have been chosen instead of C.

Formally, the probability that one alternative (say A) is chosen from a set of three alternatives {A, B, C} at a fixed time t is determined by the probability:

$$\Pr[A \mid \{A, B, C\} \text{ at time } t] = \Pr[P_A(t) > P_B(t) \ \& \ P_A(t) > P_C(t)]. \quad (6)$$

Determination of choice probabilities for choice sets with N alternatives follows the same principle outlined in Equation 6, except that it requires the conjunction of N-1 events of the form $P_A(t) > P_i(t)$, for $i \neq A$.

Dynamic Thurstone Model. On the basis of the multivariate central limit theorem, the distribution of the preference states $\mathbf{P}(t)$ converges to the multivariate normal distribution as the number of steps (t) in Equation 3 become large. If the time period between steps is small, then this convergence will occur very rapidly. Given that $\mathbf{P}(t)$ is distributed according to the multivariate normal distribution with mean $\xi(t)$ and variance-covariance matrix $\Omega(t)$, then at a fixed time point t , Equation 6 reduces to a multivariate Thurstone preferential choice model (Bock & Jones, 1968):

$$\Pr [P_A(t) - P_B(t) > 0 \ \& \ P_A(t) - P_C(t) > 0] \\ = \int_{\mathbf{X} > \mathbf{0}} \exp[- (\mathbf{X}-\Gamma)' \Lambda^{-1} (\mathbf{X}-\Gamma) / 2] / (2\pi |\Lambda|^{.5}) d\mathbf{X} \ , \quad (7)$$

where $\mathbf{X} = [P_A(t) - P_B(t), P_A(t) - P_C(t)]'$, $\Gamma = \mathbf{L}\xi(t)$, $\Lambda = \mathbf{L}\Omega(t)\mathbf{L}'$ and

$$\mathbf{L} = \begin{bmatrix} 1 & -1 & 0 \\ 1 & 0 & -1 \end{bmatrix}$$

Straightforward methods for integrating Equation 7 are described in Ashby (1992, p. 26).

Note that MDFT is a *dynamic generalization* of the classic Thurstone model, as it describes how the mean vector and variance-covariance matrix evolve systematically over time according to Equations 4 and 5. The means for each alternative, $\xi(t)$, can change signs over time so that initially one alternative (say A) may have the largest mean preference, but later another alternative (say C) may come to dominate, similar to that shown in Figure 3.

By stopping the deliberation process at various designated time points, and estimating the choice probabilities as a function of deliberation time, it is possible to observe the evolution of preferences dynamically over time. This type of externally

controlled decision paradigm already has been used successfully by cognitive researchers to study the dynamics of memory (Doshier, 1984; Hintzman & Curran, 1997; Reed, 1973). Although this method has *not* been applied to preferential choice, the present theory provides simple predictions for this type of task. Some of these predictions will be presented later during the review of the empirical results for preferential choice. The second and more frequently used type of choice task is the subject controlled choice task, which is presented next.

Subject Controlled Stopping Time

Choice tasks are called subject controlled decisions when the decision-maker is free to decide how long to deliberate before finally announcing or committing to a particular choice (cf. Ratcliff, 1978; Vickers, et.al., 1985). Considering the car purchase example, the buyer may inform the car dealer that she wishes to go home and think about the purchase, and she will call back as soon as she makes up her mind. This is the more typical type of choice task used in laboratory experiments on decision-making.

Figure 4 represents this type of choice task for the new car example. The abscissa represents deliberation time while the ordinate represents the preference state for each option. The three trajectories labeled A, B, and C represent the preferences of each option as they evolve stochastically over time according to Equation 1. The horizontal line at the top represents the threshold criterion, that is the strength of preference required to make a commitment. A choice is made as soon as the strength of preference for an option crosses the threshold, and the first option to exceed the threshold is then chosen (option B is eventually chosen in Figure 4). The time to make a decision is determined by the time required to reach the threshold bound, which is indicated by the vertical line in Figure 4.

<Insert Figure 4 about here>

The choice probabilities and decision times for the subject controlled task are determined by the first passage time distribution for a sample path to cross the threshold boundary (see Battacharya and Waymire, 1990). Formulas for computing the first passage time distribution (as well as the moments including choice probabilities and mean decision times) have been derived by Busemeyer and Townsend (1992) and Diederich (1997) for the binary choice case. At this time, the first passage time distribution for the multiple-choice (more than two alternatives) case must be obtained through computer simulation (see the Appendix B for details). This completes the presentation of the basic theory, and now we turn to several important empirical applications for multi-alternative preferential choice.

Applications to Central Empirical Findings

Similarity Effect

One of the first important results to arise from studies of preferential choice is the effect of adding a new competitive option to a choice set that has differential similarity relations to the other options in the original choice set (Sjoberg, 1977; Tversky, 1972). This effect also has significant practical implications for marketing and consumer research (Batsell & Polking, 1985; Bettman, Johnson, & Payne, 1991; Lehmann & Pan, 1994). For an example, suppose an industry considers the effect of introducing a new *competitive* product C on a market that already has two dissimilar competing products, A and B. Furthermore, suppose the new product is highly similar to product A and dissimilar to the other product B. According to the similarity effect, the introduction of the new competitive product to a choice set reduces the probability of choosing similar

products more than dissimilar products. In terms of market shares, the new product steals more of the market shares from products that are similar to it.

Figure 5 shows an example of this situation for our three-car example. The three options are represented in a two dimensional space of performance and gas mileage. Options A and B are located such that option A has better performance but poorer gas mileage than B, and option B has worse performance but better gas mileage than A. According to the similarity effect, adding a third competitive option C, that is similar to A, decreases the probability that A is chosen more than it decreases the probability that B is chosen.

<Insert Figure 5 about here>

The similarity effect leads to violations of a preferential choice property called *independence from irrelevant alternatives*. According to this property, if x and y are both elements of a choice set T which in turn is a subset of a larger choice set U , then

$$\text{if } \Pr[x / T] > \Pr[y / T], \text{ then } \Pr[x / U] > \Pr[y / U].$$

All *simple scalable* utility models must satisfy this property. The simple scalable class of choice models assumes that each alternative can be assigned a utility scale value, independent of the other alternatives in the choice set. All models in this class can be characterized by the following general formula:

$$\Pr[x | T] = F[u(x), u(y), \dots, u(z)],$$

where F is an increasing function of the first variable, and a decreasing function of the all other variables. For example, the well-known Luce (1959) choice model satisfies this property. However, the independence from irrelevant alternatives property has been shown to be systematically violated when similarity among alternatives is strongly

manipulated, and these violations rule out all models within the simple scalable class (see Tversky, 1972, for a review).

Predictions of MDFT. According to MDFT, the following intuition underlies the similarity effect. Consider the choice among options A, B, and C1 in Figure 5. Whenever attention happens to focus on the performance quality attribute, then both options A and C1 gain advantages, while option B gets a disadvantage. Likewise, whenever attention happens to focus on the gas mileage attribute, then both options A and C1 get disadvantages, while option B gains an advantage. Thus the valences of A and C1 are positively correlated with each other and negatively correlated with B. Subjects who tend to focus more on gas mileage will end up choosing option B, and subjects who tend to focus more on performance quality will end up choosing either A or C1. Thus C1 only hurts or takes away choices from option A and not B. A more formal explanation is presented below, after discussing the details about the assignment of parameters of Equation 7 to the conditions indicated in Figure 5.

According to the value structure shown in Figure 5, car A is high on performance and low on gas mileage whereas car B is just the opposite. Car C1 is similar to A but slightly better on gas mileage and slightly worse on performance. This pattern of evaluations can be represented in a simple form by the value matrix

$$M_1 = \begin{array}{cc} G & Q \\ \left[\begin{array}{cc} 1 & 3 \\ 1.25 & 2.8 \\ 3 & 1 \end{array} \right] & \begin{array}{l} A \\ C1 \\ B \end{array} \end{array}$$

The precise numerical values are not critical to produce the predicted pattern from the model, as long as the general pattern indicated in the matrix is satisfied.

The attention weights, $[w_g(t), w_q(t)]$ were assumed to fluctuate over time steps according to a simple Bernoulli process. Specifically, the probability of attending the gas mileage attribute was assigned a probability π_1 , and the probability of attending to the performance quality attribute was assigned a probability π_2 , with independent sampling across time steps (but see Footnote 1). The probability of attending to the performance attribute was set to a slightly higher level ($\pi_1 = .45$) than the probability of attending to the gas mileage attribute ($\pi_1 = .43$), and there was some small residual probability allowed for attention to irrelevant attributes. The reason for the slight difference in attention to each attribute was to produce a slight preference in favor of car A over car C1 for the binary choice condition. This was needed to satisfy the antecedent condition for the test of independence from irrelevant alternatives. The mean vector and covariance matrix for the valence, $V(t)$, was then derived from the Bernoulli process (see Appendix A for details).

The parameters for the feedback matrix were chosen as follows. First, the self – connections were set to a high value ($S_{ii} = .94$) to produce slow decay of memory. The inhibitory connections between distant alternatives were set to very low values ($S_{AB} = S_{BA} = S_{CB} = S_{BC} = -.001$). The inhibitory connections between the similar alternatives were set to relatively greater magnitudes ($S_{AC} = S_{CA} = -.025$). These parameter values satisfy the requirement for stability (i.e., the eigenvalues of S are all less than one in magnitude).

The predicted pattern does not change much as long as the inhibitory connections are not too large.

The predictions computed from Equation 7 are shown in Figure 6, which plots the probability of choice as a function of deliberation time separately for different choice alternatives. The upper and lower curves indicated with "+" and "square" symbols, respectively, represent the choice probabilities for cars A and B from the binary choice comparison. As required for the antecedent condition of the independence test, the probability of choosing A grows over time to become larger than B for the binary choice. The critical feature is revealed by the upper and lower curves indicated with a "o" and "x" symbols, respectively, representing the choice probabilities for B and A from the trinary choice comparison. Consistent with previous research, the model predicts that the probability of choosing B is higher than A for the trinary choice set, thus violating the independence from irrelevant alternatives property.

<Insert Figure 6 about here>

Note that similarity also could be manipulated by placing the new alternative C2 above and to the left of A (by slightly increasing the quality and slightly decreasing the gas mileage of C compared to A). Figure 7 shows the predictions for this case, and although the dynamics are slightly different, the model still correctly predicts the same pattern for the similarity effect.

<Insert Figure 7 about here>

It is important to understand the source of the similarity effect produced by MDFT. Interestingly, the similarity effect is *strongest* when all the inhibitory interconnections are set to *zero*. Thus lateral inhibition is not needed for the similarity

effect. However, inhibitory interconnections are needed for the other effects discussed later. To maintain consistency in our assumptions, we employed the same lateral inhibition principle across all three of the empirical applications.

According to MDFT, similarity effects are caused by the correlations among valences produced by the primary attributes. When attention is focused on the gas mileage attribute, then the valence for option B will be greater than the valences for options A and C. Alternatively, whenever attention is focused on the performance attribute, then the valence for option B will be less than the valences for options A and C. This causes the differences between B and A to be positively correlated with the differences between B and C.

Figure 8 illustrates the effects of this correlation on choice probability. The left and right panels show the equal density contours from the multivariate normal densities used in Equation 7 to compute the choice probabilities for the trinary choice set. The left panel shows the contour for option A, and the right panel shows the contour for option B. Choice probability is related to the area above and to the right of the zero preference state on the vertical and horizontal axes. Note that the strong positive correlation for option B rotates the elliptical contour into the upper right corner, thus increasing the choice probability for option B relative to A.

<Insert Figure 8 about here>

If the effect of covariance matrix for the primary attributes is attenuated, and instead, the effect of the diagonal matrix for the residual variances is accentuated (ζ), then the similarity effect disappears. This is illustrated in Figure 9, which shows the predictions of the model when the influence of ζ is increased ten fold (see Appendix A

for details). More formally, if the covariance matrix for the valence is constrained to satisfy *sphericity* (i.e., $\Phi = \sigma^2 \mathbf{I}$, producing circular contours), then the multivariate Thurstone model reduces to the Case V version, and the latter is a special case of the simple scalable class of models (cf. Bockenholt, 1992). But according to MDFT, the covariance matrix for the valence reflects the similarity structure among options in the choice set, and this implies that Φ does not satisfy sphericity.

<Insert Figure 9 about here>

Figure 10 shows a broader examination of the predictions for the similarity effect derived from MDFT. This figure shows the difference between the probability of choosing option A and the probability of choosing option B from the trinary choice set, plotted as a function of two key theoretical parameters. One parameter is the strength of the inhibitory connection between the nodes for options A and C, S_{AC} , and the second is the standard deviation of the residuals for the irrelevant attributes, ζ . The similarity effect occurs when the difference $\Pr[A|\{A,B,C\}] - \Pr[B|\{A,B,C\}]$ in the figure is negative (below the line).

<Insert Figure 10 about here>

A close look at Figure 10 shows that the similarity effect is strongest when both the standard deviation (Std) of the residuals and amount of lateral inhibition are low. Consider for example, the curve produced by the low residual Std: As the lateral inhibition increases, the effect diminishes, but one can see that even with relatively high lateral inhibition the effect is still present. Slightly increasing the residual Std when inhibition is high, however, causes the effect to disappear. Now consider the curve produced when lateral inhibition is low: As the residual Std increases, the effect

diminishes, but even at a relatively high Std one can see that the effect is still present. Under relatively high residual Std, lateral inhibition still must be increased a sizeable amount before the effect disappears. In sum, the similarity effect occurs whenever the covariance matrix for the primary dimensions ($\Phi - \zeta$) is relatively more important than the residual variance ζ . Note that experiments on the similarity effect used carefully designed stimuli that minimized the influence of irrelevant attributes in order to maximize the similarity effect.

To further check the robustness of the results across parameters and different stopping rules, the choice probabilities were also computed using the subject controlled stopping rule and slightly different parameters (see the Appendix B for details). Figure 11 shows the predictions of the model when the option C1 is added to the set already containing A and B. The ordinate shows the probability that each option (A versus B) is chosen as a function of the choice set size. The line connected with the squares represents the probabilities for choosing option A out of each set, and the line connected by the circles represents the probabilities for choosing option B out of each set. As can be seen, the probability that A is chosen relative to B is lowered when the similar option is added to the choice set, and the crossover interaction represents a violation of the independence from irrelevant alternatives property.

<Insert Figure 11 about here>

Thus far we have shown that MDFT can reproduce the well-known similarity effect under a wide variety of conditions when the valences on the primary attributes are correlated in a manner that reflects the similarity structure in the choice set. But several earlier choice models were developed to explain these results (e.g., the elimination-by-

aspects model of Tversky, 1972; and various earlier multivariate Thurstone models such as Edgell-Geisler, 1980; see also De Soute et al., 1989). The next challenge is faced by simultaneously explaining the similarity effect as well as the attraction effect. All of the above mentioned earlier models satisfy a general property known as the regularity principle. The attraction effect described next, produces empirical violations of the regularity principle.

Attraction Effect

A second important finding from studies of preferential choice is the effect of adding a new option that is *dominated* by one of the other options in the original choice set (Huber, Payne, & Puto, 1982; Ratneshwar, Shocker, & Stewart, 1987; Simonson, 1989; Weddel, 1991). For example, suppose an industry considers introducing a new product C on a market that already has two highly dissimilar competitive products, A and B. Once again, the new product C is designed to be highly similar to an older product A. But in this case, A dominates C in the sense that A is better than C on all the primary attributes. While at the same time, C neither dominates B, nor B dominates C. In this case, C is called an asymmetrically dominated decoy. The attraction effect refers to the fact that the introduction of the new *dominated* product to a choice set *increases* the probability of choosing the dominant product. In terms of market shares, the new product enhances the market share of the product that dominates it. (Note that this is just the opposite of the similarity effect produced by a new *competitive* product.)

Figure 12 illustrates this choice situation for the car purchase example. As before, Car A is superior on performance, whereas car B is superior on gas mileage. Car C is now slightly inferior on both performance and gas mileage as compared to car A. The

attraction effect refers to the empirical finding that adding C to the choice set increases the probability that option A is chosen.

<Insert Figure 12 about here>

The attraction effect produces a violation of a general principle implied by a large class of random utility models called the regularity principle (cf., Marley, 1989, Colonius, 1984). According to the regularity principle, for any option x that is an element of set T which is in turn a subset of set U, $x \in T \subseteq U$, the probability of choosing x from T must be greater than or equal to choosing x from U, $\Pr[x;T] \geq \Pr[x;U]$. In other words, the addition of option C to the set already containing A and B should only *decrease* the probability that option A is chosen (not increase it).

The regularity effect is rather robust. For example, Huber et al. (1982) investigated a variety of different choice conditions producing a wide range of binary choice probabilities. Adding the dominated decoy (C) increased the probability of choosing the dominant alternative (A) under all of these conditions. This includes (a) when A was chosen less frequently than B in a binary choice, (b) when A and B were chosen equally often in a binary choice, and (c) when A was chosen more frequently than B in a binary choice.

Predictions of MDFT. According to MDFT, the following intuition underlies the attraction effect. Consider a choice among options A, B, and C in Figure 12. Comparisons of the dominated decoy with the average of the other two options produces a negative input valence for the dominated decoy. Then this negative valence from the dominated decoy feeds through a negative inhibitory link to the closely positioned dominant option. The two negatives cancel to produce a positive bolstering effect of the

dominated decoy on the dominant option. Thus the decoy makes the dominant option "appear" stronger, similar to an edge enhancement effect in perception. A more formal explanation of the effect is provided below.

The *only* change in assignment of parameters that needs to be made for computing the predictions from Equation 7 for the attraction effect is the value matrix M (which is necessary to represent the new location of dominated option C in Figure 12). All of the remaining parameters were kept constant across the two different applications.

According to the value structure shown in Figure 12, car A is high on performance and low on gas mileage whereas car B is just the opposite. Car C is similar to A but slightly inferior on gas mileage and performance quality. This pattern of evaluations can be represented in a simple form by the value matrix

$$M_1 = \begin{array}{cc} G & Q \\ \left[\begin{array}{cc} 1 & 3 \\ .5 & 2.5 \\ 3 & 1 \end{array} \right] & \begin{array}{l} A \\ C \\ B \end{array} \end{array}$$

Once again, the precise numerical values are not critical to produce the predicted pattern from the model, as long as the general pattern indicated in the matrix is satisfied.

Figure 13 shows the predictions of MDFT for the attraction effect. The figure plots choice probability as a function of deliberation time separately for different choice alternatives. The upper and lower curves indicated with "+" and "square" symbols, respectively, represent the choice probabilities for cars A and B from the binary choice set. Similar to Figure 6, the probability of choosing A grows over time to become larger than B for the binary choice. The upper and lower curves indicated with a "x" and "o" symbols, respectively, represent the choice probabilities for A and B from the trinary

choice set. Consistent with previous research, the model correctly predicts that the probability of choosing A is higher from the trinary choice set (the "x" curve) as compared to the probability of choosing A from the binary choice set (the "+" curve), thus violating the regularity property.

<Insert Figure 13 about here >

To check the robustness of this prediction, the predictions were recomputed using Equation 7 after changing the probabilities of attending to each of the primary attributes. In one case, the probability of attending to each attribute was equated ($\pi_1 = \pi_2 = .45$), producing binary choice probabilities equal to .50 for A and B, but the probability of choosing A from the trinary set rose to .69. In another case, they were reversed ($\pi_1 = .43$, $\pi_2 = .45$) producing a binary choice probability equal to .45 for option A, but once again the probability of choosing A from the trinary set rose to .65. In both cases, the same pattern of predictions were obtained for the dominating alternative -- the decoy increased the predicted probability of choosing the dominating alternative (i.e., adding C increased the probability of choosing A) in agreement with results from Huber et al. (1982).

Note that Figure 13 was generated using exactly the same model parameters as Figures 6 and 7, except for the change in the M matrix to reflect the change of option C from a competitive to a dominated alternative close to option A. But the predicted effect of adding the dominated option (Figure 13) was just the opposite of the predicted effect of adding the competitive option (Figure 6). The theoretical reason for this dramatic change in predictions needs to be understood. If the lateral inhibitory connections are set to zero, so that the feedback matrix S is set equal to a diagonal matrix, then the attraction

effect disappears, as is shown in Figure 14. In this case, the decoy C is virtually ignored, and it has no effect on the dominating alternative A.

<Insert Figure 14 about here>

It turns out that the covariance matrix for the primary attributes does not play a crucial role for the attraction effect. Figure 15 shows the predictions when the lateral inhibition is reset to its original value but the effect of the diagonal matrix of the residual variances (ζ) is increased ten fold (using the same parameters for ζ as used in Figure 9). As can be seen in the figure, the attraction effect still occurs, although now it takes some time to build up.

<Insert Figure 15 about here>

The way that the lateral inhibition produces the enhancement effect is by gradually transforming the mean preference over time, $\xi(t)$. The dominated alternative has a below average weighted value, and when this is contrasted with the other options, its mean valence becomes negative. Then this negative mean valence from the dominated option is sent through a negative link to the dominant option, and this double negative produces a net positive input to the dominant option. In this way, the dominated option C bolsters the dominant option A. Option B does not enjoy any bolstering because it is too dissimilar to A, and the inhibitory connection is too weak to produce the effect.

In sum, lateral inhibitory connections are crucial and covariance structure is less important for MDFT to produce the attraction effect. The concept of lateral inhibition has been used in perception to explain phenomenon such as edge enhancement effect and mach bands (Grossberg, 1988). In much the same way as lateral inhibition explains edge

enhancement effects, here it explains how adding a dominated decoy enhances the probability that A is chosen relative to B.

Figure 16 shows a more detailed examination of the predictions for the attraction effect derived from MDFT. This figure shows the difference between the probability of choosing option A from the trinary set and the probability of choosing A from the binary set, plotted as a function of the two key theoretical parameters: The strength of the inhibitory connection between the nodes for options A and C, S_{AC} , and the standard deviation of the residuals for the irrelevant attributes, ζ . The decoy effect occurs when the difference $\Pr[A|\{A,B,C\}] - \Pr[A|\{A,B\}]$ in the figure is positive (above the line).

<Insert Figure 16 about here>

A close look at Figure 16 shows that the attraction effect is strongest when the standard deviation (Std) of the residuals is low and amount of lateral inhibition is high. Consider for example, the curve produced by the low residual Std: As the lateral inhibition increases, the effect quickly becomes present and increases dramatically with increasing amounts of lateral inhibition. Now consider the curve produce when lateral inhibition is low: When the residual Std is low the effect is not present, and increasing residual Std does not lead to the occurrence of the effect. In sum, lateral inhibition is much more critical to explaining the attraction effect than is amount of residual Std.

A complete explanation for similarity and attraction effects must include a formal explanation for their intricate interactions. The next section considers the effects of varying the position of the decoy on similarity and attraction effects.

Similarity and Attraction Interactions

Distance effects. A fundamental implication of the lateral inhibitory explanation for the attraction effect is that it should diminish with psychological distance between the decoy and the dominant option. For example, consider moving the decoy from position C gradually down to position D in Figure 12. According to MDFT, this movement increases the distance between the decoy and dominant option, causing the lateral inhibition between the decoy and the dominant option to decrease. MDFT predicts that the bolstering effect of the decoy should gradually attenuate and finally be eliminated after moving from positions C to D.

Table 1 illustrates this effect, where the results are computed from Equation 7 using the same parameters as in Figure 13, except for the changes indicated in the table. The first column represents the value of the decoy option on the performance attribute, and the second column represents the lateral inhibition from A to C. The last two columns show the probabilities of choosing option A from the binary and trinary choice sets. The first and last rows represent positions C and D, respectively, in Figure 12, and the intermediate rows represent positions between C and D. As can be seen in the table, the attraction effect gradually disappears with distance. In agreement with this prediction, the attraction effect has been empirically found to decrease and eventually disappear with increasing distance (Heath & Chatterjee, 1991; Wedell, 1991).

<Insert Table 1 about here>

Range vs. Frequency Decoys. A more refined prediction can be tested by considering the differential effects of decoys R versus F shown in Figure 12. The range decoy, R, is dominated by A because it has the same performance but worse gas mileage than A. It is called a range decoy because adding it to the choice set increases the range

on the gas mileage dimension. The frequency decoy, F , is dominated by A in that it has the same gas mileage as A but worse performance. It is called a frequency decoy because adding it to the choice set increases the frequency of items below A . Using range and frequency decoys, Huber et al. (1982) found that the decoy effect was stronger with range decoys as compared to frequency decoys.

According to MDFT, changing the position of the decoy changes the similarity of the decoy to option B . Notice in Figure 12 that the range decoy is further away from B than the frequency decoy. The principle of lateral inhibition states that inhibition decreases as a function of distance. This implies that the inhibitory connection between nodes for options F and B is stronger than the inhibitory connections between nodes for options R and B .

The above explanation for the differences between range and frequency decoys was verified by computing the predictions of MDFT using different inhibitory connections in the S matrix for range and frequency decoys. Furthermore, to check the robustness of the theory's predictions concerning the dominant decoy effect, the subject controlled stopping rule was used to compute the probabilities for this application (but note that similar results are obtained using Equation 7). For the range decoy, the following S matrix shown was used:

$$S = \begin{array}{c} \begin{array}{ccc} A & R & B \end{array} \\ \left[\begin{array}{ccc} .95 & -.09 & -.001 \\ -.09 & .95 & -.003 \\ -.001 & -.003 & .95 \end{array} \right] \begin{array}{l} A \\ R \\ B \end{array} \end{array}$$

For the frequency decoy, a slightly different S matrix was used:

$$S = \begin{array}{c} \begin{array}{ccc} A & F & B \end{array} \\ \left[\begin{array}{ccc} .95 & -.09 & -.001 \\ -.09 & .95 & -.02 \\ -.001 & -.02 & .95 \end{array} \right] \begin{array}{l} A \\ F \\ B \end{array} \end{array}$$

Notice the only difference between these two matrices is the inhibition between the decoy and B. For the range decoy the value was -.003 and for the frequency decoy it was -.02. Once again, referring to Figure 12, these numbers reflect the fact that F is closer to B than is R. Thus, the only change needed to capture the different effects of range versus frequency decoys was a change in lateral inhibition that reflects the distances of the objects in attribute space.

Figure 17 shows the predictions of MDFT under various choice conditions for range and frequency decoys. The abscissa represents the probability that the dominating option (A) is chosen from a binary choice set. The ordinate represents the probability that A is chosen out of a trinary choice set that includes a decoy. Each point in the figure represents a pair of probabilities $[\Pr(A|\{A,B\}), \Pr(A|\{A,B,C\})]$ obtained from the same choice condition. The line connected by circles represents the probability that A is chosen when the frequency decoy was presented for various choice conditions. The line connected by the triangles represents the probability that A is chosen when the range decoy was presented for various choice conditions. The identity line connected by the squares represents the probability that A is chosen in the binary condition. (This was included to facilitate the comparisons between binary and trinary choice probabilities.)

<Insert Figure 17 about here>

In Figure 17, the regularity principle requires all of the points to lie on or below the identity line. Violations of regularity occur when any of the points appear above the identity line. As can be seen in Figure 17, the model predicts that adding either a frequency or a range decoy produces violations of regularity across the entire range of

binary choice probabilities. Furthermore, the range decoy has a larger effect as compared to the frequency decoy, consistent with the findings of Huber, et al. (1982).

Inferior Decoys. A final test MDFT is obtained by considering the effect of adding what is called an inferior decoy to the choice set. For example, consider the decoy labeled "I" in Figure 12. Technically, this is a competitive option because it is superior to option A on performance quality. Practically, however, it is inferior to option A because the small advantage in terms of performance is offset by a large disadvantage in terms of gas mileage. Inferior decoys are like dominated decoys in the sense that they are rarely ever chosen. Huber & Puto, (1983) examined the effects of inferior decoys and found that they produced attraction effects similar to dominated decoys.

Note that if option "I" shown in Figure 12 is shifted horizontally over to the right toward the position of option C2 in Figure 5, then the inferior option changes into a highly competitive option. Huber & Puto, (1983) also examined the effect of gradually changing the inferior option into a competitive option in this manner. They found that the proportion of choices for option A decreased, the proportion of choices for option "I" increased, but the proportion of choices for option B changed very little. In other words, both attraction and similarity effects were demonstrated within the same study.

These interactions are precisely the effects expected from MDFT. Table 2 shows the results at time $t = 100$ computed from Equation 7 using the same parameters as used to produce Figure 6 and Figure 13, except for changes in the value of gas mileage for the inferior option. The first column shows the gradual shifts in the value of the gas mileage attribute from .85 (i.e., the value used to define option C2 in Figure 5) to .55 (i.e., the value used to define option "I" in Figure 12). The second and third rows show the

probabilities of choosing options A and B from the trinary choice set {A, B, I}. As can be seen in the table, decreasing the gas mileage drastically increased the probability of choosing option A, while the probability for B changed very little. Also note that an attraction effect is produced by the inferior option when the gas mileage was relatively low in value. These predictions are in accord with the findings by Huber and Puto (1983).

<Insert Table 2 about here>

Although earlier choice models have been proposed specifically to account for the attraction effect (e.g., Ariely & Wallsten, 1995; Dhar & Glazer, 1996), only MDFT has been simultaneously applied to both the similarity and attraction effects and their interactions. Furthermore, these earlier models never attempted to formally explain another finding known as the compromise effect described next.

Compromise Effect

A third important finding from studies of preferential choice is the effect of adding a new option that lies *between* two competing extreme options in the original choice set (Simonson, 1989; Simonson & Tversky, 1992; Tversky & Simonson, 1993). Suppose there are three equally attractive products A, B, and C, as indicated by their pairwise preferences. But suppose two of the products, say A and B, are extremely different, and the third product is a compromise that lies in between these two extremes. The compromise effect refers to the empirical finding that when all three options are available for choice, the compromise is chosen more frequently than either of the extremes. Unlike the previous decoy effect, the attractiveness of the compromise option is enhanced by introducing a new competitive (as opposed to dominated) option.

Figure 18 illustrates this choice situation for the car purchase example. As before, Car A is superior on performance, whereas car B is superior on gas mileage. Car C is a compromise lying in between these two extremes – C is not as good as A on performance but better than A on gas mileage, while at the same time, C is not as good as B on gas mileage but better than B on performance. The compromise effect refers to the empirical finding that

$$\Pr[A|\{A,B\}] = \Pr[A|\{A,C\}] = \Pr[B|\{B,C\}], \text{ but}$$

$$\Pr[C|\{A,B,C\}] > \Pr[A|\{A,B,C\}] \text{ and } \Pr[C|\{A,B,C\}] > \Pr[B|\{A,B,C\}].$$

In other words, the compromise is enhanced when viewed within the context of the two extremes. Furthermore, the effect is found even when the trinary choice set is presented *before* the three binary comparisons (and thus the result is not due to new information about options that change the attribute space).

<Insert Figure 18 about here>

Predictions of MDFT. The experimental conditions used to produce the compromise effect required a few changes in model parameters. First, the values in the matrix M were changed to represent the new location of compromise option C in Figure 18 as follows. According to the value structure shown in Figure 18, car A is high on performance and low on gas mileage whereas car B is just the opposite. Car C is in between these two being inferior to B on gas mileage and inferior to A on performance quality. This pattern of evaluations can be represented in a simple form by the value matrix

$$M = \begin{array}{cc} & \begin{array}{c} G \quad Q \end{array} \\ \begin{array}{c} \left[\begin{array}{cc} 1 & 3 \\ 2 & 2 \\ 3 & 1 \end{array} \right] & \begin{array}{c} A \\ C \\ B \end{array} \end{array}$$

Once again, the precise numerical values are not critical to produce the predicted pattern from the model, as long as the general pattern indicated in the matrix is satisfied.

The inhibitory connections in the feedback matrix also need to be changed to reflect the equal distances between the compromise option and the two extreme options. The self connections were set to $S_{ii} = .94$, the inhibitory connections between the two extreme options were set to $S_{AB} = S_{BA} = -.001$, and the inhibitory connections between the compromise and each extreme were set to $S_{AC} = S_{CA} = S_{CB} = S_{BC} = -.025$. Note that all these parameters are exactly the same as those used to produce the decoy effect in Figure 15. The only difference is that the inhibitory connections between A and C are now set to the same values as the inhibitory connections between C and B, reflecting the fact that the compromise is placed in between the two extremes.

Finally, the probability of attending to the performance quality attribute was set equal to the probability of attending to the gas mileage dimension ($\pi_1 = \pi_2 = .45$). This was necessary to meet the antecedent conditions for the compromise effect. Using these parameters forced all of the binary choice probabilities equal to .50. The remaining model parameters used to compute the predictions from Equation 7 were assigned exactly the same values as those used to produce the attraction effect shown in Figure 15.

Figure 19 shows the predictions of MDFT for the compromise effect. The figure plots choice probability as a function of deliberation time separately for different choice alternatives. The upper curve indicated with a "+" symbol represent the choice

probability for the compromise car C out of the trinary choice set. The overlapping two lower curves represent the choice probabilities for the two extreme options, A and B, from the trinary choice set. The choice probabilities from the binary choice set are not shown because all three are exactly equal (.50). Figure 19 shows that the probability of choosing the complement alternative, C, grows over time to become larger than both A and B. Consistent with previous research, the model correctly predicts that the probability of choosing the compromise from the trinary set is higher than the extremes, despite the fact that the binary choice probabilities are all equal to .50.

<Insert Figure 19 about here>

Once again, lateral inhibition is crucial for producing this effect. If the lateral inhibitory interconnections are eliminated, then the predicted compromise effect disappears. But the explanation is quite different from that used to explain the attraction effect. Lateral inhibition does not bolster the mean preference of the compromise alternative because *all three* options were assigned equally attractive weighted values. The *mean* valence input is zero for all, and multiplication of the feedback matrix, S , by the zero mean input produces zero mean output, and thus the mean preference state remains at zero over time.

The source of the effect lies in the operation of lateral inhibition on the *momentary fluctuations* in valence. The negative inhibitory connections between the nodes for the compromise and extreme options cause the compromise to be negatively correlated with both of the extremes. This in turn causes the differences between the compromise and extreme option A to be positively correlated with the difference between

the compromise and extreme option B. Finally, the positive correlation for the compromise provides a probabilistic advantage over the extreme option in Equation 7.

The probabilistic advantage produced by the positive correlation can be seen in Figure 20. The left and right panels show the equal density contours from the multivariate normal densities used in Equation 7 to compute the choice probabilities for the trinary choice set. The left panel shows the contour for an extreme option (e.g., A), and the right panel shows the contour for the compromise option C. Choice probability is related to the area above and to the right of the zero preference state on the vertical and horizontal axes. Note that the relatively stronger positive correlation for the compromise rotates the elliptical contour further into the upper right corner, thus increasing the choice probability for the compromise option.

<Insert Figure 20 about here>

Figure 21 shows a more detailed examination of the predictions for the compromise effect derived from MDFT. This figure shows the difference between the probability of choosing option C over A from the trinary set, plotted as a function of the two key theoretical parameters: The strength of the inhibitory connection between the nodes for options A and C, S_{AC} , and the standard deviation of the residuals for the irrelevant attributes, ζ . The compromise effect occurs when the difference $\Pr[C|\{A,B,C\}] - \Pr[A|\{A,B,C\}]$ in the figure is positive (above the line).

A close look at Figure 21 shows that the compromise effect is strongest when both the standard deviation (Std) of the residuals and amount of lateral inhibition are high. Consider for example, the curve produced by high residual Std: When lateral inhibition is high, the effect is present and as the lateral inhibition diminishes, the effect

disappears. Now consider the curve produce when lateral inhibition is high: With low residual Std the effect is not present, but as the residual Std increases, the effect quickly becomes present and continues to increase with residual Std. With relatively low lateral inhibition, increasing residual Std cannot produce the effect. In sum, the compromise effect occurs whenever the lateral inhibition and residual Std are not both very low. It is worth noting that studies investigating the compromise effect have typically employed realistic stimuli permitting a sizeable contribution from irrelevant attributes.

<Insert Figure 21 about here>

To check the robustness of the predictions for MDFT, the predictions were computed again using the subject controlled stopping rule and slightly different parameters (see Appendix B for details). The parameters were assigned in a manner to guarantee that all three binary choice probabilities were equal to .50. The results for the trinary choice set produced the same pattern of results as shown in Figure 19: The probability of choosing the compromise (.48) exceeded the probability of choosing either the upper extreme alternative A (.27) or the lower extreme alternative B (.25).

The compromise effect occurs when the compromise option hurts or takes away shares equally or symmetrically from both extreme alternatives (Simonson and Tversky, 1992; Tversky and Simonson, 1993). However, not all stimuli were precisely designed to produce this symmetry. Simonson and Tversky (1992) also reported unequal or asymmetric effects, called polarization effects, in which the compromise hurt one extreme more than the other extreme. The polarization effect also can be accommodated within MDFT by relaxing the assumption that the psychological distances between the compromise option and each extreme option are *exactly* equal. To demonstrate a

polarization effect, the trinary choice probabilities are recomputed from Equation 7 using the exactly the same parameters as used in Figure 19 with the following single exception. The inhibitory connection between option C and B was changed to $S_{BC} = -.01$ (slightly less than the inhibitory connection $S_{AC} = -.025$ between option C and A). The results for the binary choices were unchanged, and the results at time $t = 100$ for the trinary set produced a polarization effect. The compromise C is chosen with probability .35, the extreme option A is chosen with the same probability .35, but the probability of choosing the other extreme B was reduced to .30. Thus, allowing asymmetry in the lateral inhibition connections reproduces the polarization effect reported by Simonson and Tversky (1992).

Although a formal theory already has been developed to explain the compromise effect (Tversky & Simonson, 1993), there are several advantages to be claimed for MDFT over this earlier theory. First, this earlier theoretical treatment never attempted to formally address the interactions between similarity and attraction discussed above. Second, Tversky & Simonson's (1993) theory is essentially an extension of the classic weighted additive utility model (with contextually dependent weights). In contrast, MDFT is a dynamic and stochastic choice model capable of providing quantitative predictions for choice probability as a function of deliberation time. For example, Figure 19 indicates that the compromise effect should not occur under short time limits, and it only appears after there is sufficient time for the lateral inhibition effects to build up. In sum, MDFT produces interesting dynamic predictions for multiple alternative choice, some of which are examined in more detail below.

Effects of time pressure

Consumer decisions take time and the time taken to make a purchase can influence the final choice. For example, suppose a consumer is considering the purchase of a new product that is slightly inferior to an older standard product on the most important attribute (e.g., money), but superior on other secondary attributes (quality, looks, performance, etc.). If a salesperson presses the consumer into a quick decision, then this time pressure may force the decision to be based on limited information, possibly only the most important attribute, thus minimizing the likelihood of purchasing the new product. Alternatively, if the salesperson encourages the consumer to deliberate longer and consider more of the secondary attributes, then the likelihood of a choice in favor of the new product would slowly rise over time. This type of preference reversal under time pressure has been experimentally verified in several recent multi-attribute preference experiments (Diederich; 1997; Svenson and Edland, 1993). Findings such as these underscore the importance of decision time for predicting choice behavior.

The multi-attribute version of decision field theory developed by Diederich (1997) explained preference reversals under time pressure on the basis of shifts in attention to attributes over time. However, the current development indicates another important source for changes in preference under time pressure – the effects of lateral inhibition need time to build up before they can influence choice probability.

In particular, the dynamics of lateral inhibition have important implications for the effects of deadline time pressure on violations of regularity produced by the dominated decoy. The model predictions based on the dynamic Thurstone model (Equation 7) shown in Figures 13 and 15 indicate that the decoy effect needs time to

build up. In other words, MDFT makes the counterintuitive prediction that time pressure decreases the likelihood of violating the regularity principle of preferential choice.

To examine the predictions of MDFT in more detail, new predictions were obtained using the more commonly used subject controlled stopping rule. According to decision field theory, time pressure causes a reduction in the threshold boundary – the boundary is assumed to be an increasing function of the time limit. Under low time pressure (long time limits) a high bound is employed, which allows preferences to accumulate to a stronger preference level for a longer average deliberation time. Under high time pressure, a lower bound is employed, which forces the process to stop early and decide on the basis of a weak strength of preference.

Predictions were computed for the decoy effect using the same parameters as used in Figure 17, except that the position of the threshold boundary was varied. Figure 22 shows the predictions of the model for the decoy effect as a function of the threshold boundary (time limit). The abscissa represents boundary placement while the ordinate represents the probability of choosing A, the dominating alternative. The line connected with squares represents the probability that A is chosen in the binary choice conditions. In this case, the parameters were fixed to produce an equal probability of choosing A or B. The line connected by diamonds reflects the probability that A is chosen with the decoy present. Notice that with high time pressure (short time limit and small boundary), the model predicts that regularity will be satisfied. This is reflected in Figure 22 (as well as Figure 15) in that with high time pressure, adding the decoy decreases the probability that A is chosen. However, as time pressure decreases (time limit and boundary increases), the model predicts regularity will be violated. This is reflected in Figure 22 (as

well as Figure 15) in that with low time pressure, adding the decoy increases the probability that A is chosen. According to MDFT, this interaction effect occurs because with high time pressure, choices are made too quickly, not allowing time for the lateral inhibition to build up.

<Insert Figure 22 about here>

Although more rigorous tests of this hypothesis are underway, preliminary evidence supports the general idea that attraction effects increase with longer deliberation times. First, Wedell (1993) found attraction effects to be positively correlated with choice response time. Second, Simonson (1989) reported that attraction effects are enhanced when subjects are motivated to carefully deliberate about their decisions.

Pre-decisional Search

It is commonly accepted among decision researchers that different decision strategies are employed, depending on the number of alternatives presented in the choice set (cf., Payne, Bettman, & Johnson, 1993; Wright & Barbour, 1977). At the beginning, when a large number of alternatives are being considered, a simple elimination process is used to quickly screen out options that are unacceptable on the first couple of attributes. Later, when only a few competitive options remain after this initial screening, a more deliberative compensatory process is used to make the final selection. For example, consumers may start by using an elimination-by-aspects type of choice rule (Tversky, 1972) and then later switch to a weighted additive difference rule (Tversky, 1969).

A large amount of evidence has accumulated over the past 20 years for strategy-switching dependent on choice set size (see Payne et al., 1993). One index used to monitor strategies is the proportion of information searched, defined as the ratio of the

number of cells considered out of the total the number of cells available within an alternative by attribute value matrix. This index has been found to decrease as the choice set size increases. Another important index is the direction of search, defined as the ratio $(\text{within attribute comparisons} - \text{between attribute comparisons}) / (\text{within attribute comparisons} + \text{between attribute comparisons})$. This index has been found to increase as the choice set size increases. Both of these findings are consistent with the idea of strategy switching from a quick elimination process to a more thorough compensatory process as the choice set size decreases. Other process measures based on eye movements and memory recall of values also support this general idea (see; Russo & Rosen, 1975; Levin & Jasper, 1995).

In this section, we show how MDFT mimics strategy-switching simply by adding a second, lower, elimination boundary to the subject controlled stopping rule.² Previous applications of the subject controlled stopping rule considered only the case where there was an upper accept boundary. Now consider the case where there is only a lower reject boundary and no upper acceptance boundary. Figure 23 illustrates an example for a hypothetical deliberation process involving five new cars that are evaluated along three attributes. The abscissa represents time and the ordinate represents preference. The lower reject boundary is placed at -50 in the figure. Each line represents the evolution of preferences computed from Equation 1 for a particular car option over time. The vertical lines represent shifts of attention from one attribute to another during the deliberation process. In this case, the first attribute is gas mileage, the second comfort, and the third performance. As can be seen, while focusing on the first attribute, gas mileage, two options (B, E) were eliminated from the choice set. With the shift to the second attribute,

comfort, no items were eliminated. However, with the shift to the third attribute, performance, two more options (C, D) were eliminated. Finally, the choice is based on the last remaining option (A).

<insert Figure 23 about here>

The complete version of this decision process employs both an upper acceptance boundary and a lower rejection boundary. The lower boundary represents the criterion level of preference used to reject options from consideration. The upper boundary represents the criterion level of preference used to select an option as the final choice. But in this case, there are two ways an option can be chosen: One is to be the first to cross the upper boundary (stopping the search), and if that fails for all options, then the other is to be the last to survive rejection.

The double boundary version of MDFT can mimic strategy-switching by allowing the lower reject boundary to change depending on the number of options initially presented to the decision maker. When the choice set is large, the lower boundary is set equal to a small distance below the neutral point (zero preference state), thus allowing quick rejection of inferior alternatives, and only allowing superior alternatives to survive further consideration. When the choice set is small, then lower bound is set farther below the neutral point to avoid eliminating any option too quickly, and every alternative receives thorough consideration. In general, the criterion for rejecting becomes more lenient (closer to neutral) as the choice set size increases.

To show how this simple idea mimics strategy-switching phenomena, a simulation was performed using the choice sets presented in one of the original pre-decisional processing studies by Payne, Braunstein, & Carroll (1978). In this study

subjects were presented 2, 7, or 12 alternatives described by 12 attributes, with one of three (low, medium, or high) evaluations assigned to each alternative - attribute cell. Furthermore, the alternatives were constructed so that each alternative was high on four attributes, medium on four, and low on four, and the distribution varied across alternatives so that no alternative dominated another.

One thousand simulated subjects were run on the above multiple choice task using Equation 1 to generate the preferences, and double boundaries to make the final decision (see Appendix B for details). The criterion for rejection was set to high, medium, and low magnitudes for the 2, 7, and 12 alternative choice sets, respectively. The main results for this simulation are shown in Figure 24. The ordinate represents the probability that an option is rejected, conditioned on the event that it is not already rejected (i.e., number of options rejected divided by the number of options still remaining). The abscissa represents the number of attributes that have been processed during deliberation on a choice set. The steeply declining curve shows the results produced by the 12-alternative choice set, the flat curve shows the results for the 2-alternative choice set, and the intermediate curve shows the results for the 7-alternative choice set.

<Insert Figure 24 about here>

For the 12-alternative set, the majority of options are rejected very quickly on the basis of comparisons within only the first or second attributes. For example, the probability of rejecting any one of the 12 options on the basis of the first attribute is .45, and the probability of rejecting an option on second attribute (given that it survived the first attribute) is .40. On the average, 8 out of 12 alternatives are eliminated on the basis of the first two attributes alone. But as the number of attributes processed in increases,

the probability of rejection rapidly declines, so that the probability of rejecting any one of the superior options that survive until the seventh attribute is only .10 and this rejection probability gradually approaches zero. Thus the two-boundary model behaves like an elimination process when a large number of alternatives are available in the choice set.

For the 2-alternatives set, the likelihood of eliminating an option is very small. In this case, the probability of rejection remains approximately constant at a very low average level equal to .01 across the 12 attributes. The probability that each option survives past the first 11 attributes is approximately .90. This allows time to consider all of the trade-offs between the two alternatives very carefully and thoroughly on the basis of a very large number of attributes before reaching a decision.

Using these simulation results, we also can compute the indices for the two main pre-decisional search measures mentioned earlier. The proportion of information search is a decreasing function of the rejection rate, and the rejection rate increases with choice set size. For this simulation, the proportion of information searched decreased from a high level of .89 for the 2-alternative set, to .45 for the seven alternative set, down to a low level of .25 for the 12-alternative set. The basic trend for the direction of search is to increase the proportion of within attribute comparisons as the choice set size increases. For this simulation, the direction of search index increased from .38 for the 2-alternative set, to .79 for the 7 alternative set, and up to .89 for the 12 alternative choice set. This agrees qualitatively with the basic pattern of findings from previous research.

Summary of Empirical Applications.

Thus far we have shown that MDFT provides a uniform and comprehensive account of the critical empirical findings from multi-alternative preferential choice

studies. This includes explanations for similarity effects, attraction effects, compromise effects and their subtle interactions. Our examination of the theoretical basis for these effects yields some interesting relations between the theoretical parameters and the effect sizes. First, we found that relatively low lateral inhibition and residual Std facilitate the similarity effect, whereas relatively high lateral inhibition and residual Std facilitate the compromise effect. High inhibition also facilitates the attraction effect, but the residual Std plays a minor role. Secondly, based on response surface analyses, it is apparent that massive regions of the parameter space (i.e., combinations of lateral inhibition and residual Std) exist where all these effects are expected. Finally, a tentative prediction may be made concerning individual differences. Individuals showing the strongest similarity effect may evince weaker compromise effects and vice versa. Thus there should be a negative correlation between attraction effects and similarity effects, as opposed to a positive correlation between the attraction and compromise effects. Results supporting these individual difference predictions have been reported by Wedell (1993).

MDFT also explains findings related to the dynamical aspects of the decision process. A directly testable prediction derived from the present theory is that both the attraction effect and the compromise effect should be attenuated by time pressure. In contrast, the similarity effect is not expected to decrease under time pressure, and instead this effect should remain fairly constant across time. Thus MDFT predicts qualitatively different effects of time pressure on choice probability for the three major findings. Although a formal test of this hypothesis remains to be performed, preliminary evidence supports the general idea that attraction effects increase with longer deliberation times (Simonson, 1989; Wedell, 1993).

Finally, we showed how MDFT assimilates findings regarding the pre-decisional search processes used to filter a large set of options down to a smaller competitive set. By employing both an upper acceptance boundary and a lower rejection boundary, MDFT can emulate findings regarding pre-decisional search processes reported in the literature. Specifically, at the beginning, when a large number of alternatives are being considered, a simple elimination process is used to quickly screen out options that are unacceptable on the first couple of attributes. Later, when only a few competitive options remain after this initial screening, a more deliberative compensatory process is used to make the final selection. The last section compares MDFT with earlier theories of multi-alternative preferential choice.

Comparisons with Other Models

Decision Theories. During the past 20 years, decision theorists have made significant theoretical progress toward the development of theories for preferential choice. Some models were successful for explaining the similarity effect (Tversky, 1972; Edgell-Geisler, 1980; Candel, 1997; see also De Soute et al., 1989), while others were successful for explaining the attraction effect (Ariely & Wallsten, 1995; Dhar & Glazer, 1996) or the compromise effect (Tversky & Simonson, 1993). But up to this point, a common formal theoretical explanation for all three pivotal effects has eluded past researchers. In particular, models specifically designed to explain similarity effects couldn't explain violations of regularity resulting from the attraction effect. Similarly, models specifically designed to explain attraction effects lack formal explanations for violations of independence from irrelevant alternatives produced by the similarity effect. As the previous sections show, MDFT succeeds in providing a coherent explanation for

all three classes of phenomena as well as the subtle interactions among these effects. For example, not only does MDFT provide an explanation of the main effect for the dominated decoy, but it also accounts for differences between range and frequency decoys and the positions of inferior decoys on the attraction effect.

There are also major theoretical differences between previous decision theories of preferential choice and MDFT. The former class of models lacks any type of process description (an exception is the elimination by aspects model). Consequently, they are not equipped to describe pre-decisional search processes and how they change with choice set size. Furthermore, the static nature of the former class of models prohibits any predictions regarding the effects of time pressure or time limits on decision making. MDFT is a dynamic-stochastic model capable of explaining the relations between choice probability and decision time as well as pre-decisional search characteristics.

Neural Networks. Several neural network models of decision making have recently been proposed that are also dynamic in nature. Levin and Levine (1996) proposed a multi-attribute neural network decision model to explain consumer choice behavior, however it was not applied to any of the major empirical findings on multi-alternative preferential choice discussed here. Another dynamic model proposed by Usher and Zakay (1993) was designed to implement an elimination-by-aspects choice process using a neural network framework. It succeeds in providing an explanation of the similarity effect, however, like the elimination-by-aspects model, no explanations for the attraction effect and the compromise effect follow from this theory. Thus its fair to say that MDFT provides a more comprehensive account of the main findings than both of the previous neural network models do.

Theoretically there are some similarities and differences between the earlier neural network models and MDFT. All share a common assumption that recurrent interconnections are important for explaining the evolution of preference over time. However, only MDFT relates the lateral interconnections to the distance between alternatives in the multi-attribute value space. Additionally, there are two other major differences between the models. One concerns the stochastic nature of choice behavior. The earlier models generate choice probabilities by varying initial states across choice trials, whereas MDFT assumes that the inputs to the system vary stochastically over time within each choice trial. The latter approach is more widely accepted and successfully used in cognition (e.g., Ratcliff, 1978; Smith, 1995). A second major difference concerns the nature of the dynamics. The earlier models are nonlinear, whereas MDFT is linear. The obvious theoretical advantage gained by using linear dynamics is simplicity, which allows us to derive closed form solutions for the choice probabilities as a function of decision time (see Equation 7, also see Busemeyer and Townsend, 1992, and Diederich, 1997, for the binary choice - subject controlled stopping rule). Eventually, evidence may come forth that compels us to generalize from linear to nonlinear dynamics. But until that time, parsimony demands retention of the linear dynamics.

Implications for Future Research. MDFT not only provides a more complete explanation of the major findings from past research on multi-alternative choice than previous theories, but it also generates new testable predictions and provides new directions for research. For example, MDFT predicts that the compromise effect should gradually turn into a similarity effect as the compromise option is moved along the diagonal toward one of the extreme options in Figure 18 (analogous to the similarity –

attraction interactions shown in Table 2). Another interesting prediction is that the attraction effect results from a build up of lateral inhibition, and therefore it should take time to build. Although preliminary evidence supports the latter hypothesis (Simonson, 1989; Wedell, 1993), more rigorous tests are required to rule out possible explanations based on random guessing under time pressure. We are currently beginning a new program of research to examine these and other predictions from MDFT. Several experimental tests of predictions derived from the original version of decision field theory have recently appeared, and the results were found to be in agreement with theory (see Diederich & Busemeyer, in press; Dror, Busemeyer, & Basala, in press). The goal of the present article is to lay down the basic theoretical foundation for future model tests and model comparisons.³

Conclusion

We have recast decision field theory (Busemeyer & Townsend, 1993) into a neural network framework and extended it to encompass multi-alternative decision-making. Two earlier important theories (weighted additive utility, Thurstone choice theory) were shown to be derivable as special cases of our theory. The central thrust of the study then probed MDFT relative to three essential experimental findings concerning multi-choice situations, the similarity effect, the attraction effect, and the compromise effect. MDFT is the only formal and quantitatively specified theory that has successfully explained all three effects, and other future testable predictions were considered. In addition, we demonstrated that MDFT can simulate behavior associated with Tversky's elimination-by-aspects process and discussed the critical time-orientated facets and potential predictions of MDFT. Finally, we compared MDFT with other multi-alternative

choice models, in particular with those possessing neural network interpretations.

Decision field theory is based on a simple set of theoretical assumptions, all of them founded on long-standing psychological principles in motivation, decision-making, and information processing. Over the past several years, it has begun to demonstrate itself to be capable of explaining a broad spectrum of classical results and making new testable predictions, many of which have been investigated and confirmed. The present work suggests that major multi-alternative choice phenomena naturally ensue from the extended theory.

References

- Ariely, D. & Wallsten, T. S. (1995). Seeking subjective dominance in multidimensional space: An exploration of the asymmetric dominance effect. *Organizational Behavior and Human Decision Processes*, 63(3), 223-232.
- Aschenbrenner, K. M., Albert, D., & Achmalhofer, F. (1984). Stochastic choice heuristics. *Acta Psychologica*, 56(1-3), 153-166.
- Ashby, F. G. (1992). Multidimensional models of perception and cognition. Hillsdale, NJ: Erlbaum.
- Batsell, R. R. & Polking, J. C. (1985) A new class of market share models. *Marketing Science*, 4, 177-198.
- Bettman, J. R., Johnson, E. J. & Payne, J. W. (1991). Consumer decision making. In T. S. Robertson & H. H. Kassirjian (Eds.) *Handbook in Consumer Behavior*. Englewood Cliffs, NJ: Prentice-Hall. (Pp. 50-84).
- Bhattacharya, R. N., & Waymire, E. C. (1990). Stochastic processes with applications. New York: Wiley.
- Bock, R. D., & Jones, L. V. (1968). The measurement and prediction of judgment and choice. San Francisco, CA: Holden-Day.
- Bockenholt, U. (1992). Multivariate models of preference and choice. In F. G. Ashby (Ed.)
- Bussemeyer, J. R. & Townsend, J. T. (1992). Fundamental derivations from decision field theory. *Mathematical Social Sciences*, 23, 255-282.

Busemeyer, J. R. & Townsend, J. T. (1993). Decision Field Theory: A dynamic cognition approach to decision making. *Psychological Review*, 100, 432-459.

Candel, M. J. J. M. (1997). A probabilistic feature model for unfolding tested for perfect and imperfect nestings. *Journal of Mathematical Psychology*. 41(4), 414-430.

Colonius, H. (1984). *Stochastische theorien individuellen wahlverhaltens*. Berlin: Springer-Verlag.

De Soute, G. Feger, H. & Klauer, K. C. (Eds.) (1989). *New developments in probabilistic choice modeling*. Amsterdam: North Holland.

Dhar, R. & Glazer, R. (1996) Similarity in context: Cognitive representations and violation of preference and perceptual invariance in consumer choice. *Organizational Behavior and Human Decision Processes*, 67, 280-293.

Diederich, A. (1997). Dynamic stochastic models for decision making under time constraints. *Journal of Mathematical Psychology*, 41(3), 260-274.

Diederich, A. & Busemeyer, J. R. (in press) Conflict and the stochastic dominance principle of decision making. *Psychological Science*.

Dosher, B. A. (1984). Discriminating pre-experimental (semantic) from learned (episodic) associations: A speed accuracy study. *Cognitive Psychology*, 16(4), 519-555.

Dror, I. E., Busemeyer, J. R., & Basola, B. (In press) Decision Making Under Time Pressure: An independent test of sequential sampling models. *Memory and Cognition*.

Edgell, S. E. & Geisler W. S. (1980) A set-theoretic random utility model of choice behavior. *Journal of Mathematical Psychology*, 21(3), 265-278.

Grossberg, S. (1988). *Neural Networks and Natural Intelligence*. Cambridge, M.A.:MIT Press.

Grossberg, S. & Gutowski, W. E., (1987). Neural dynamics of decision making under risk: Affective balance and cognitive-emotional interactions. *Psychological Review*, 94(3), 300-318.

Heath, T. B. & Chatterjee, S. (1991) How entrants affect multiple brands: A dual attraction mechanism. *Advances in Consumer Research*, 18, 768-771.

Hintzman D. L. & Curran, T. (1997). Comparing retrieval dynamics in recognition memory and lexical decision. *Journal of Experimental Psychology: General*, 126(3), 228-247.

Huber, J., Payne, J. W., & Puto, C. (1982). Adding asymmetrically dominated alternatives: Violations of regularity and the similarity hypothesis. *Journal of Consumer Research*, 9(1), 90-98.

Huber, J. & Puto, C. (1983) Market boundaries and product choice: Illustrating attraction and substitution effects. *Journal of Consumer Research*, 10, 31-44.

Keeney, R. L. & Raiffa, H. (1976). *Decisions with multiple objectives: Preference and value tradeoffs*. New York: John Wiley & Sons

Lehmann, D. R., & Pan, Y. (1994) Context effects, new brand entry, and consideration sets. *Journal of Marketing Research*, 31, 364-374.

Levin, I.P. & Jasper, J. D. (1995) Phased narrowing: A new process tracing method for decision making. *Organizational Behavior and Human Decision Processes*, 64, 1-8.

Levin, S. J., & Levine, D. S. (1996). Multiattribute decision making in context: A dynamic neural network methodology. *Cognitive Science*, 20, 271-299.

Lewin, K. (1935). *A dynamic theory of personality*. New York:McGraw-Hill.

Luce, R. D. (1959). *Individual choice behavior: A theoretical analysis*. New York: Wiley, 1959.

Marley, A. A. J. (1989). Random utility family that includes many of the 'classical' models and has closed form choice probabilities and choice reaction times. *British Journal of Mathematical and Statistical Psychology*, 42, 13-36.

Mellers, B. A., Schwartz, A., & Cooke, D. J. (1998). Judgment and decision making. *Annual Review of Psychology*, 49, 447-477.

Payne, J. W., Bettman, J. R., & Johnson, E. J. (1992) Behavioral decision research: A constructive processing perspective. *Annual Review of Psychology*, 43, 87-131.

Payne, J. W., Braunstein, M. L., & Carroll, J. S. (1978). Exploring predecisional behavior: An alternative approach to decision research. *Organizational Behavior and Human Decision Processes*, 22(1), 17-44.

Ratcliff, R. (1978). A theory of memory retrieval. *Psychological Review*, 85(2), 59-108

Ratneshwar, S., Shocker, A. D., & Stewart, D. W. (1987) Toward understanding the attraction effect: The implications of product stimulus meaningfulness and familiarity. *Journal of Consumer Research*, 13, 520-527.

Reed, A. V. (1973). Speed-accuracy tradeoff in recognition memory. *Science(Washington, D.C.)*, 181, 574-576.

Rumelhart, D. E., & McClelland, J. L. (1986). *Parallel distributed processing Explorations in the microstructure of cognition. Vol. 1: Foundations*. Cambridge, MA: MIT Press.

Russo, J. E. & Rosen, L. D. (1975) An eye fixation analysis of multialternative choice. *Memory and Cognition*, 3, 267-276.

Samuelson, W. & Zeckhauser, R. (1988). Status quo bias in decision making. *Journal of Risk and Uncertainty*, 1, 7-59.

Simon, H. A. (1955). A behavioral model of rational choice. *Quarterly Journal of Economics*, 69, 99-118.

Simonson, I. (1989) Choice based on reasons: The case of attraction and compromise effects. *Journal of Consumer Research*, 16, 158-174.

Simonson, I. & Tversky, A. (1992) Choice in context: Tradeoff contrast and extremeness aversion. *Journal of Marketing Research*, XXIX, 281-295.

Sjoberg, L. (1977). Choice frequency and similarity. *Scandinavian Journal of Psychology*, 18, 103-115.

Smith, P. L. (1995). Psychophysically principled models of visual simple reaction time. *Psychological Review*, 102(3), 567-593

Svenson, O. & Edland, A. (1987). Change of preferences under time pressure: Choices and judgments. *Scandinavian Journal of Psychology*, 28, 322-330.

Takane, Y. (1989). Analysis of covariance structures and probabilistic binary choice data. In De Soute, G. Feger, H. & Klauer, K. C. (Eds.) *New developments in probabilistic choice modeling*. Amsterdam: North Holland. (Pp. 139-160).

Thurstone, L. L. (1959). *The measurement of values*. Chicago: University of Chicago Press.

Townsend, J. T., & Busemeyer, J. R. (1995) Dynamic representation of decision-making. In R. F. Port and T. van Gelder (Eds.) *Mind as Motion*. MIT press.

Tversky, A. (1969). Intransitivity of preferences. *Psychological Review*, 76, 31-48.

Tversky, A. (1972). Elimination by aspects: A theory of choice. *Psychological Review*, 79(4), 281-299.

Tversky, A. & Simonson, I. (1993). Context dependent preferences. *Management Science*, 39, 1179-1189.

Usher, M. & Zakay, D. (1993). A neural network model for attribute-based decision processes. *Cognitive Science*, 17(3), 349-396.

Vickers, D., Burt, J., Smith, P., & Brown, M. (1985). Experimental paradigms emphasizing state or process limitations: I. Effects of speed^accuracy tradeoffs. *Acta Psychologica*, 59(2), 129-161.

Von Winterfeldt, D. & Edwards, W. (1986). *Decision analysis and behavioral research*. Cambridge: Cambridge University Press.

Wedell, D. H. (1991). Distinguishing among models of contextually induced preference reversals. *Journal of Experimental Psychology*, 17, 767-778.

Wedell, D. H. (1993). Studying effects of different decoys on choice in a within-subject design. Paper presented at the Annual meeting of the Society for Judgment and Decision Making.

Wright, P. & Barbour, F. (1977). Phased decision strategies: Sequels to an initial screening. In M. Starr & M. Zeleny (Eds.) Multiple criteria decision making: TIMS studies in the management sciences. Amsterdam: North-Holland.

Appendix A

Details for Figures 6, 7, and 9. The attention weights for the two primary attributes were assumed to fluctuate according to a simple Bernoulli process with probabilities $\pi_1 = .43$ and $\pi_2 = .45$. Based on this assumption, we derive $W_I = E[W_I(t)] = [\pi_1 \ \pi_2]'$, and $\Psi = \mathbf{diag}(W_I) - W_I W_I'$. The values for the M_I matrix described in the text were then inserted to compute $\mu = CM_I W_I$ and $\Phi = CM_I \Psi M_I' C' + \zeta$, where ζ was initially set to $\zeta = \mathbf{diag}(.1, .1)$ for Figures 6 and 7, but it was set to $\zeta = \mathbf{diag}(10, 10)$ for Figure 8. These matrices were then inserted into Equation 7 to produce the predictions shown in Figures 6, 7, and 9.

Appendix B

Binary Choice Probabilities

At each time step the preference vector for each alternative was updated using the C matrix for binary choice given in the text and the following S matrix in Equation 1:

$$S = \begin{bmatrix} .95 & 0 \\ 0 & .95 \end{bmatrix}.$$

Attention shifted between dimensions in that at each time step, with a probability of .5, a column of the M matrix was chosen for use in updating the preference vector. Once a column was chosen, an error vector distributed $N(0, 7)$ was added to represent momentary fluctuations in value. The simulation continued until the preference for one option reached an upper boundary of 60. The option that reached the boundary first was

the option chosen for that simulated subject. One thousand subjects were simulated for each effect. These same procedures, with the same parameters, were used in all trinary simulations with the exception of the **M**, **C**, and **S** matrices.

Similarity

Simulations were run exactly as with the binary case discussed above except with different **M**, **C**, and **S** matrices. The following **M** matrix was used:

$$M_1 = \begin{array}{cc} & \begin{array}{c} G \quad Q \end{array} \\ \begin{array}{c} A \\ B \end{array} & \begin{bmatrix} 28.2 & 12.2 \\ 29 & 11 \\ 10 & 30 \end{bmatrix} \end{array} \textit{Similar}$$

This matrix was chosen such that the values for A and B led to a slight advantage for choosing of A over B in the binary case. The C matrix was the same as that presented in the text. The following S matrix was used:

$$S = \begin{array}{ccc} & \begin{array}{c} A \quad S \quad B \end{array} \\ \begin{array}{c} A \\ S \\ B \end{array} & \begin{bmatrix} .95 & -.09 & -.001 \\ -.09 & .95 & -.003 \\ -.001 & -.003 & .95 \end{bmatrix} \end{array}$$

Values in this matrix were chosen to take into account the relative positions of the options in the multi-attribute evaluation space. For example, the lateral inhibition between A and S is greater than A and B due to the fact that it is closer in space (see Figure 5).

Attraction Effect

Simulations for the attraction effect were exactly the same as for the similarity effect except for the differences in the **M** and **S** matrices. The **M** matrices were chosen such that there was a range of probabilities of choosing A over B in the binary case.

$$\begin{array}{ccc}
 P(A|A,B)=.25 & P(A|A,B)=.5 & P(A|A,B)=.75 \\
 \\
 \begin{array}{cc} G & Q \\ \left[\begin{array}{cc} 22 & 18 \\ 17.6 & 18 \\ 31 & 10 \end{array} \right] & M_1 = \begin{array}{cc} G & Q \\ \left[\begin{array}{cc} 22 & 18 \\ 17.6 & 18 \\ 30 & 10 \end{array} \right] & \\ \\ M_1 = \begin{array}{cc} G & Q \\ \left[\begin{array}{cc} 23 & 18 \\ 18.4 & 18 \\ 30 & 10 \end{array} \right] & \end{array}
 \end{array}
 \end{array}$$

Also, there was a slight variation in the **S** matrices to reflect the relative distances of the decoys in the multi-attribute evaluation space

$$\begin{array}{ccc}
 \text{S matrix for Range Decoy} & & \text{S matrix for Frequency Decoy} \\
 \\
 \begin{array}{ccc} A & R & B \\ \left[\begin{array}{ccc} .95 & -.09 & -.001 \\ -.09 & .95 & -.003 \\ -.001 & -.003 & .95 \end{array} \right] \begin{array}{l} A \\ R \\ B \end{array} & & \begin{array}{ccc} A & F & B \\ \left[\begin{array}{ccc} .95 & -.09 & -.001 \\ -.09 & .95 & -.02 \\ -.001 & -.02 & .95 \end{array} \right] \begin{array}{l} A \\ F \\ B \end{array}
 \end{array}
 \end{array}$$

The rationale for the values in these matrices is given in the text.

Compromise Effect

Simulations for the compromise effect were exactly the same as the decoy effect with different **M** and **S** matrices.

$$\begin{array}{ccc}
 \begin{array}{cc} G & Q \\ \left[\begin{array}{cc} 15 & 25 \\ 20 & 20 \\ 25 & 15 \end{array} \right] \begin{array}{l} A \\ C \\ B \end{array} & & \begin{array}{ccc} A & C & B \\ \left[\begin{array}{ccc} .95 & -.05 & -.001 \\ -.05 & .95 & -.05 \\ -.001 & -.05 & .95 \end{array} \right] \begin{array}{l} A \\ C \\ B \end{array}
 \end{array}
 \end{array}$$

Values in the **M** matrix were chosen to coincide with their positions in the multi-attribute evaluation space. The **S** matrix was chosen to have equal lateral inhibition between A and C and B and C also due to their positions in the multi-attribute evaluation space.

Search Variability

Values for the **M** matrix were chosen such that each option had 12 attributes, four of which had a high value, four medium, and four low (1, 0, -1 respectively). Attribute values were ordered such that no option dominated another. Simulations were run separately for one of three choice set sizes, 2, 7, 12. Hence, for the 12 option set, the original **M** matrix was a 12 (#options) x 12 (# attributes) matrix with each row representing values across dimensions for each alternative. For the 7 and 2 option sets the **M** matrix was constructed similarly and were of size 7 x 12 and 2 x 12 respectively.

Because some options are eliminated from the choice set during deliberation, the size of all of the matrices changed. The **S** matrix consisted of a # options remaining x # options remaining diagonal matrix with .95 on the diagonal and zeros everywhere else. The **C** matrix was constructed to compare the each alternative with the average of all other alternatives.

The upper preference boundary to choose an option was set at 50. The lower boundary to discard an option was set at -30, -20, -10 for the 2, 7, and 12 option sets respectively. Attention shifted from one dimension to another in that on each trial there was a 95% probability that the same dimension would be used at the next time step and a

5% probability of moving to the next dimension. An error component of $N\sim(0,7)$ was added to the column of the M matrix chosen on each trial. Simulations were run for each subject until an option crossed the upper boundary, all but one option was discarded, or all 12 dimensions were cycled through.

Author Notes

This research was supported by a NIMH grant F321MH11988-02 to the first author, and grants NIMH Perception and Cognition R01 MH55680 and NSF Decision Risk Management Science SBR-9602102 and James McKeen Cattell Fellowship to the second author. The authors would like to thank Rob Goldstone for his comments on an earlier version of this work.

Footnotes

¹ In this application we assume that the attention weights are identically and independently distributed over time according to a simple Bernoulli process. However, Diederich's (1997) multi-attribute decision field model employs a more sophisticated Markov process for switching attention to attributes. The Bernoulli process is a simple special case of the more general Markov process, but it is sufficient for the present purposes.

² Ratcliff (1978) introduced the idea of using a lower reject bound to eliminate items in his earlier retrieval model of recognition memory.

³ Unfortunately most of the data from previous experiments are not suitable for quantitative tests due to the small number of experimental conditions and the small sample sizes within each condition. For this reason we have considered only the qualitative predictions of MDFT. Quantitative tests of decision field theory have been performed in other applications (e.g., Busemeyer & Townsend, 1993; Dror, et. al., in press), and new experiments are underway to provide both qualitative as well as quantitative tests of time pressure and attraction effects.

Table 1. Effect of increasing the distance between decoy option and dominant option on the size of the attraction effect.

Value on Performance	A-C inhibition	$\Pr(A A,B)$	$P(A A,B,C)$
2.5	-.025	.55	.73
1.5	-.01	.55	.66
.75	-.003	.55	.58
.50	-.001	.55	.55

Table 2: Effect of Inferior option on trinary choice probabilities

Gas mileage for I	Pr[A A, B, I]	Pr[B A, B, I]
.85	.33	.43
.75	.50	.42
.65	.57	.40
.55	.61	.38

Note: The first column refers to the value of the M matrix corresponding to the first attribute, gas mileage, for the inferior option "I." The first row corresponds to the position of option "C2" in Figure 5, and the last row corresponds to the position of option "I" in Figure 12. The 2nd and 3rd rows correspond to positions of inferior alternatives shifted horizontally along the line from "I" to "C2". The binary choice probability of choosing A over B was uniformly equal to .55 for all rows.

Figure Captions

Figure 1. First stage of MDFT consisting of a feed-forward network. The output of this stage, valences (V), are formed by filtering the evaluation (M) of each option through momentary attention weights (W) and then comparing those values with other options (C).

Figure 2. Second stage of MDFT consisting of a recursive network. The output of this stage, preferences (P), are formed by recursively comparing the valences for each option node labeled A, B, and C using weights given in connections matrix S.

Figure 3. An example of an externally controlled choice process. The abscissa represents time while the ordinate represents level of preference. The three trajectories labeled A, B, and C represent the preferences of each option as they evolve stochastically over time according to Equation 1. The vertical line to the right represents the appointed time for the decision. In this case, the option with the highest preference at the designated time point is the one chosen.

Figure 4. An example of a subject controlled choice process. The three trajectories labeled A, B, and C represent the preferences of each option as they evolve stochastically over time according to Equation 1. The horizontal line at the top represents the threshold criterion, that is the strength of preference required to make a commitment. A choice is made as soon as the strength of preference for an option crosses the threshold

Figure 5. Examples of competitive similar alternatives for the three car example. The abscissa represents the dimension of gas mileage while the ordinate represents the dimension of performance. Squares labeled A and B indicate the original options and C1 and C2 indicate two competitive options similar to option A.

Figure 6. MDFT predictions for the similarity effect. The probability of choice is plotted as a function of deliberation time separately for different choice alternatives. The upper and lower curves indicated with "+" and "square" symbols, respectively, represent the choice probabilities for cars A and B from the binary choice comparison. The upper and lower curves indicated with a "o" and "*" symbols, respectively, representing the choice probabilities for B and A from the trinary choice comparison using similar alternative C1 from Figure 5.

Figure 7. Predictions of MDFT for similarity effect using similar alternative C2. Axes are the same as Figure 6.

Figure 8. A graph showing the effects on choice probability of correlation among valences produced by the primary dimensions. The left and right panels show the equal density contours from the multivariate normal densities used in Equation 7 to compute the choice probabilities for the trinary choice set. The left panel shows the contour for option A, and the right panel shows the contour for option B. Choice probability is related to the area above and to the right of the zero preference state on the vertical and horizontal axes.

Figure 9. Predictions of MDFT when the influence of diagonal matrix for the residual variances is increased (ζ increased ten fold. Axes the are same as Figure 6.

Figure 10. A graph showing the difference between the probability of choosing option A and the probability of choosing option B from the trinary choice set plotted as a function of two key theoretical parameters. One parameter is the strength of the inhibitory connection between the nodes for options A and C, S_{AC} , and the second is the standard deviation of the residuals for the irrelevant attributes, ζ . The similarity effect occurs when the difference $P(A|A,B,C) - P(B|A,B,C)$ in the figure is negative (below the line).

Figure 11. Results of simulations of the similarity effect using the subject controlled stopping rule. The ordinate shows the probability that each option (A versus B) is chosen as a function of the choice set size. The line connected with the squares represents the probabilities for choosing option A out of each set, and the line connected by the circles represents the probabilities for choosing option B out of each set.

Figure 12. Examples of dominated decoy alternatives for the three car example. The abscissa represents the dimension of gas mileage while the ordinate represents the dimension of performance. Squares labeled A and B indicate the original options and R, F, and C indicate three options dominated by option A.

Figure 13. A plot of the MDFT predictions for the dominated decoy effect. Choice probability is plotted as a function of deliberation time separately for different choice alternatives. The upper and lower curves indicated with "+" and "square" symbols, respectively, represent the choice probabilities for cars A and B from the binary choice set. The upper and lower curves indicated with a "*" and "o" symbols, respectively, represent the choice probabilities for A and B from the trinary choice set

Figure 14. A plot of the MDFT predictions for the dominated decoy effect when the effect of lateral inhibition is removed. Axes are labeled the same as in figure 13.

Figure 15. A plot of the MDFT predictions for the dominated decoy effect when the influence of the diagonal matrix of residual variances is increased ten fold. Axes are labeled the same as in Figure 13.

Figure 16. A more detailed examination of the predictions for the decoy effect derived from MDFT. This figure shows the difference between the probability of choosing option A from the trinary set and the probability of choosing A from the binary set, plotted as a function of the two key theoretical parameters: The strength of the inhibitory connection between the nodes for options A and C, S_{AC} , and the standard deviation of the residuals for the irrelevant attributes, ζ . The decoy effect occurs when the difference $P(A|A,B,C) - P(A|A,B)$ in the figure is positive (above the line).

Figure 17. A plot showing results of simulations of MDFT under various choice conditions for range and frequency decoys. The abscissa represents the probability that the dominating option (A) is chosen from a binary choice set. The ordinate represents the probability that A is chosen out of a trinary choice set that includes a decoy. Each point in the figure represents a pair of probabilities $[P(A|\{A,B\}), P(A|\{A,B,C\})]$ obtained from the same choice condition. The line connected by circles represents the probability that A is chosen when the frequency decoy was presented for various choice conditions. The line connected by the triangles represents the probability that A is chosen when the range decoy was presented for various choice conditions. The identity line connected by the squares represents the probability that A is chosen in the binary condition

Figure 18. Example of a compromise alternative for the three car example. The abscissa represents the dimension of gas mileage while the ordinate represents the dimension of performance. Squares labeled A and B indicate the original options while C indicates the compromise option.

Figure 19. Predictions of MDFT for the compromise effect. Choice probability is plotted as a function of deliberation time separately for different choice alternatives. The upper curve indicated with a "+" symbol represent the choice probability for the compromise car C out of the trinary choice set. The overlapping two lower curves represent the choice probabilities for the two extreme options, A and B, from the trinary choice set.

Figure 20. A graph showing the effects on choice probability of correlation among valences produced by the primary dimensions. The left and right panels show the equal density contours from the multivariate normal densities used in Equation 7 to compute the choice probabilities for the trinary choice set. The left panel shows the contour for an extreme option (e.g., A), and the right panel shows the contour for the compromise option C. Choice probability is related to the area above and to the right of the zero preference state on the vertical and horizontal axes.

Figure 21 A more detailed examination of the predictions for the compromise effect derived from MDFT. The difference between the probability of choosing option C over A from the trinary set, is plotted as a function of the two key theoretical parameters: The strength of the inhibitory connection between the nodes for options A and C, S_{AC} , and the standard deviation of the residuals for the irrelevant attributes, ζ . The compromise effect occurs when the difference $P(C|A,B,C) - P(A|A,B,C)$ in the figure is positive (above the line).

Figure 22 Predictions of the MDFT for the decoy effect as a function of the threshold boundary (time limit). The abscissa represents boundary placement while the ordinate represents the probability of choosing A, the dominating alternative. The line connected with squares represents the probability that A is chosen in the binary choice conditions.

Figure 23 An illustration of the essential ideas for a hypothetical deliberation process involving five new cars that are evaluated along three attributes. The abscissa represents

time and the ordinate represents preference. Each line represents the evolution of preferences computed from Equation 1 for a particular car option over time. The vertical lines represent shifts of attention from one attribute to another during the deliberation process. The first attribute is gas mileage, the second comfort, and the third performance.

Figure 24 Strategy switching as a function of choice set size. The ordinate represents the probability that an option is rejected, conditioned on the event that it is not already rejected (i.e., number of options rejected divided by the number of options still remaining). The abscissa represents the number of attributes that have been processed during deliberation on a choice set. The steeply declining curve shows the results produced by the 12-alternative choice set, the flat curve shows the results for the 2-alternative choice set, and the intermediate curve shows the results for the 7-alternative choice set.

Figure 1

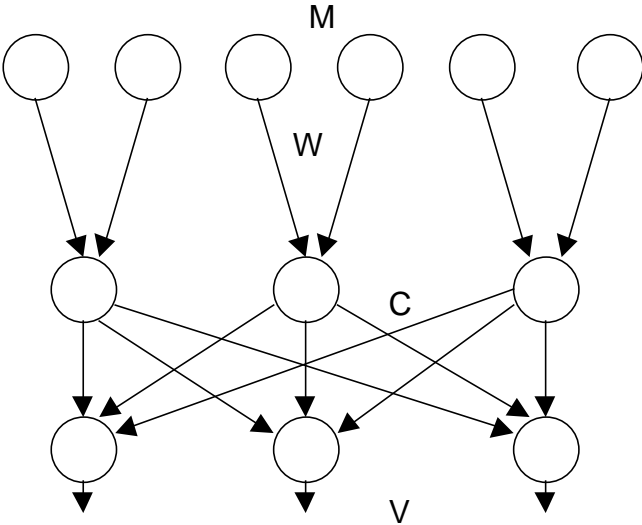


Figure 2

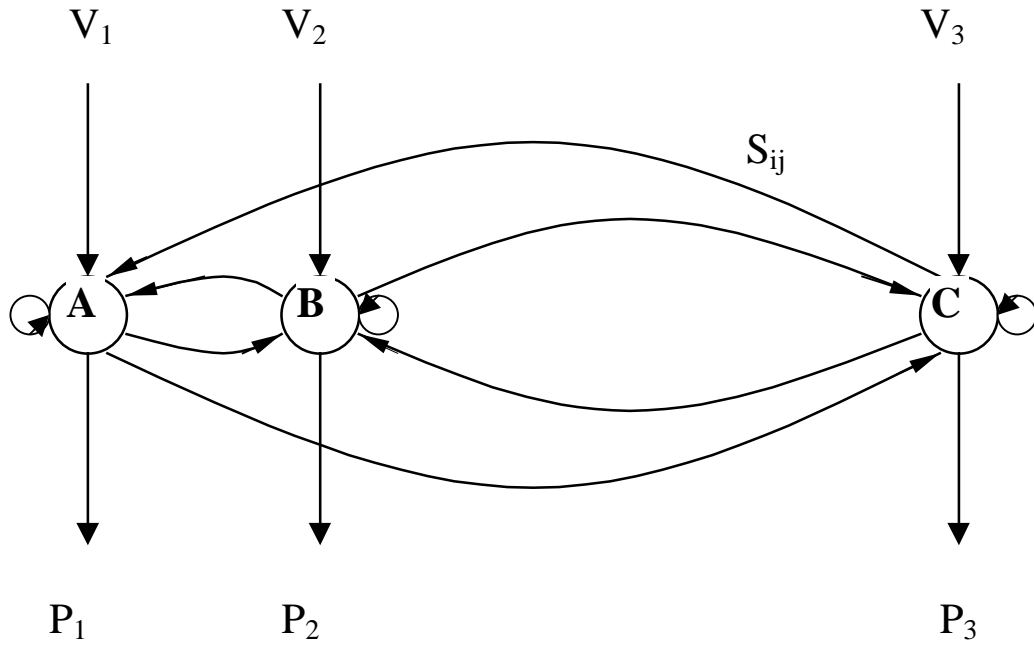


Figure 3

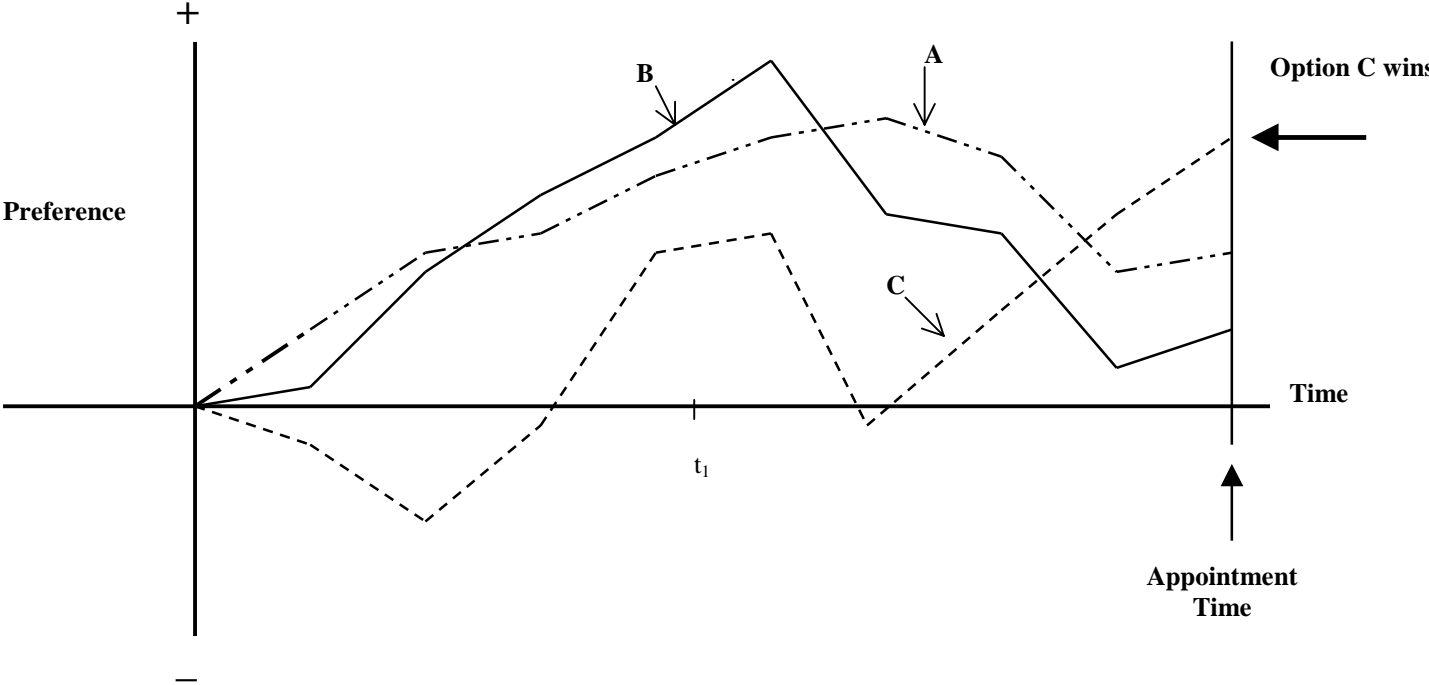


Figure 4

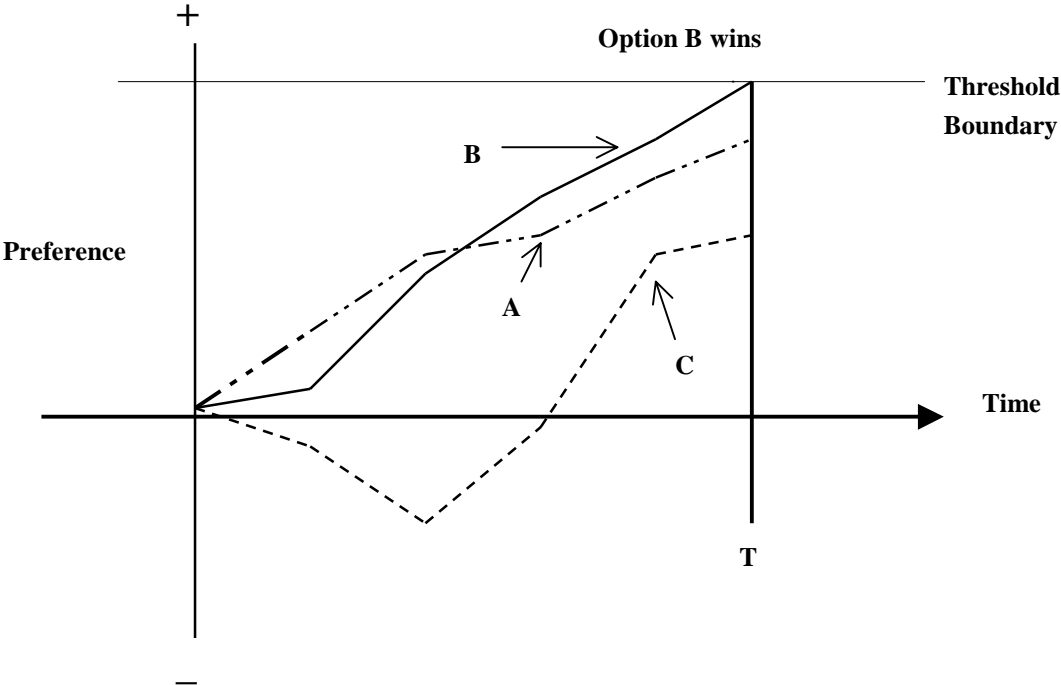


Figure 5

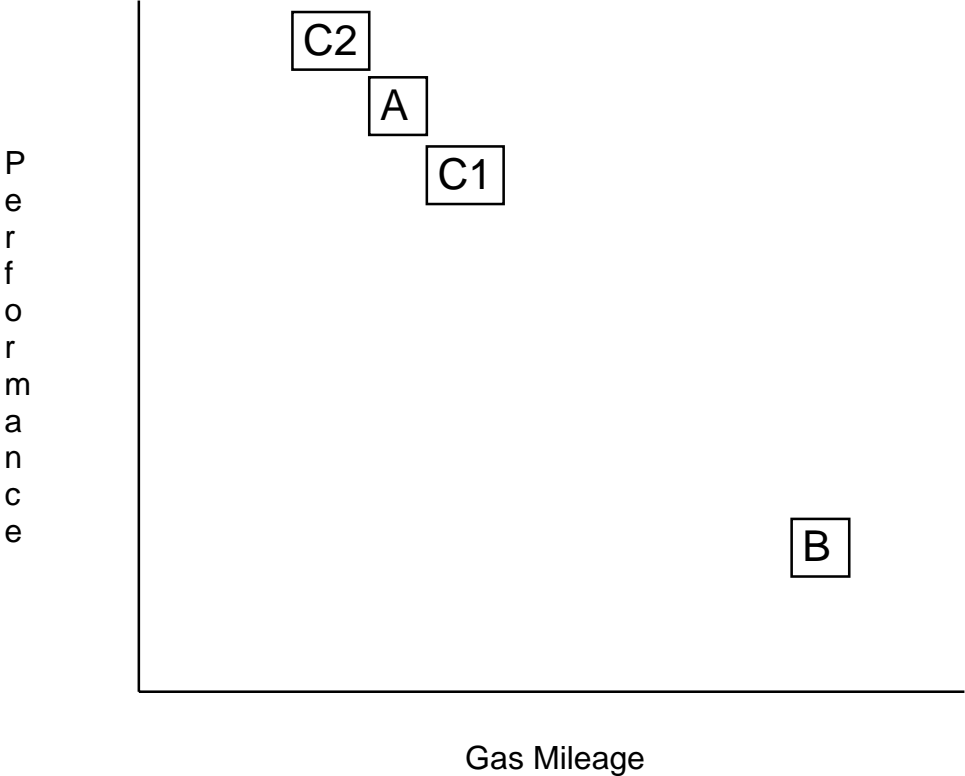


Figure 6 (C1)

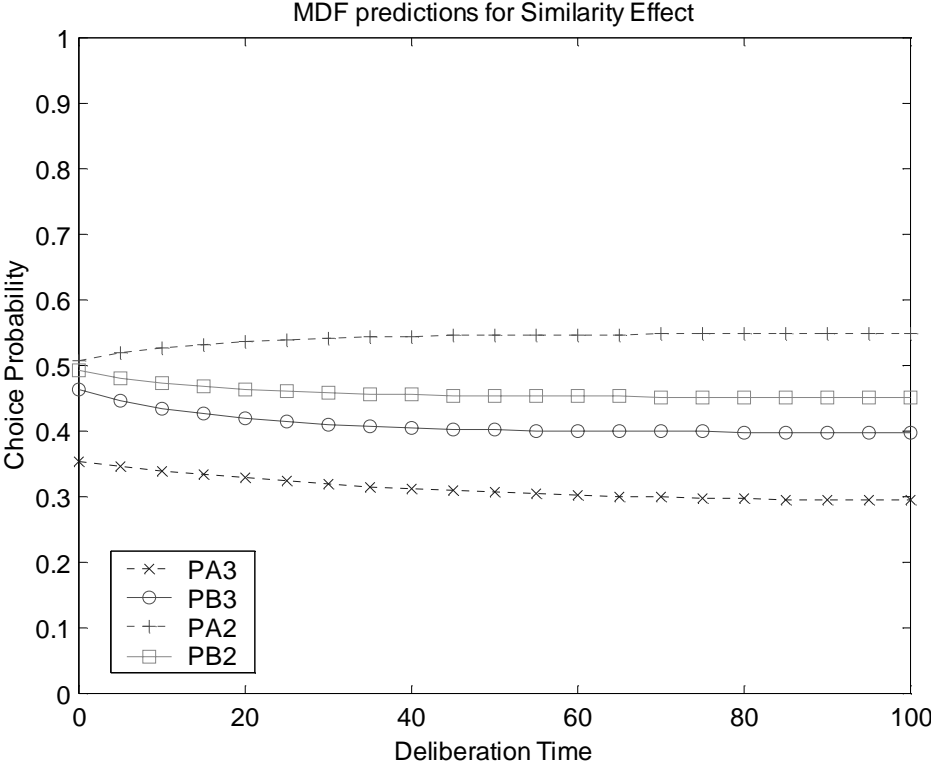


Figure 7 (C2)

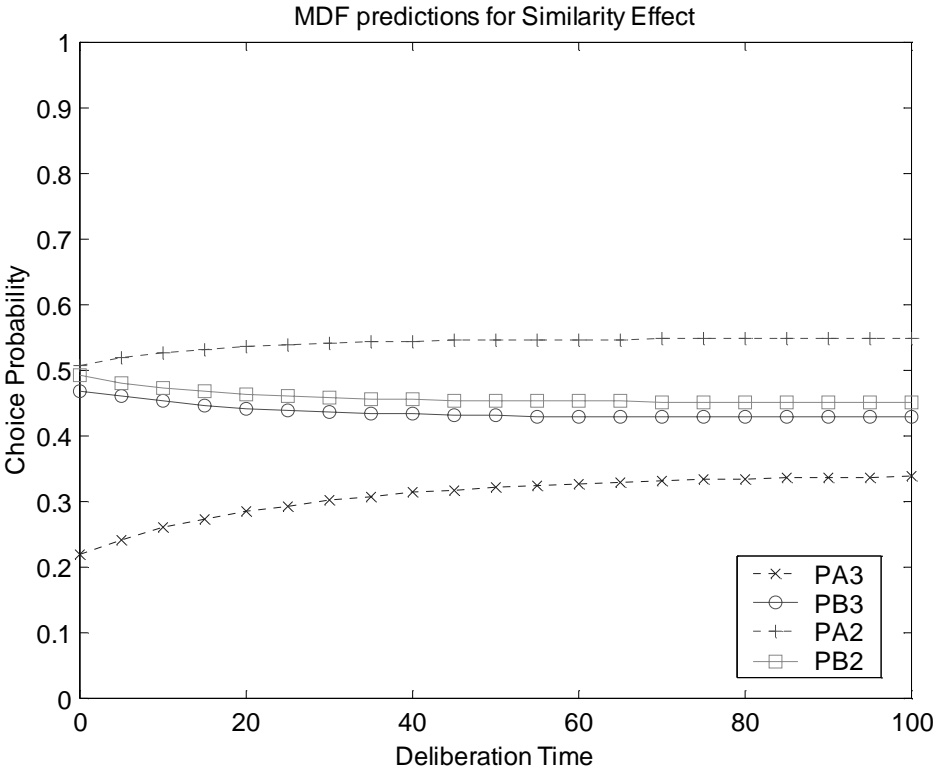


Figure 8 (C2)

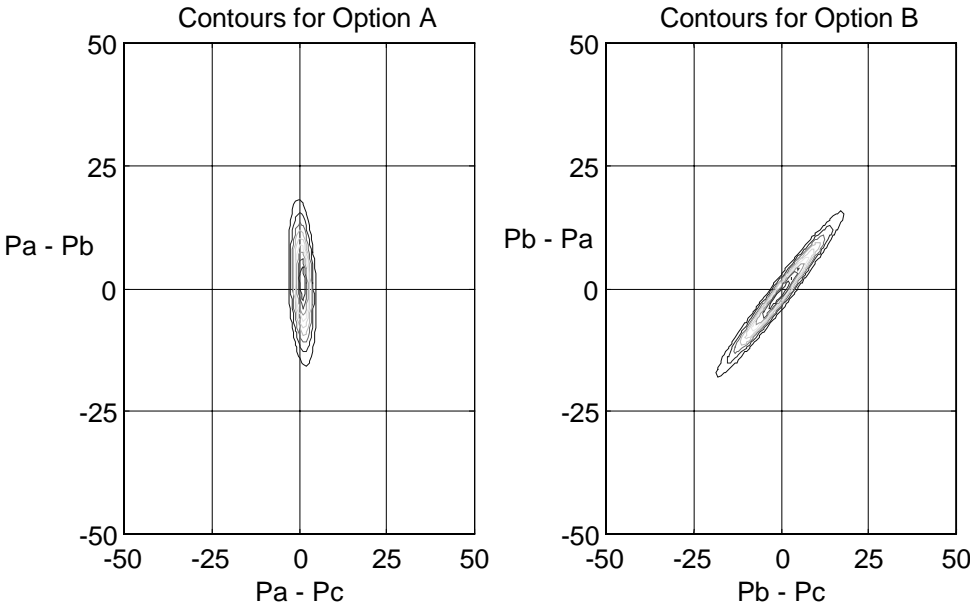


Figure 9

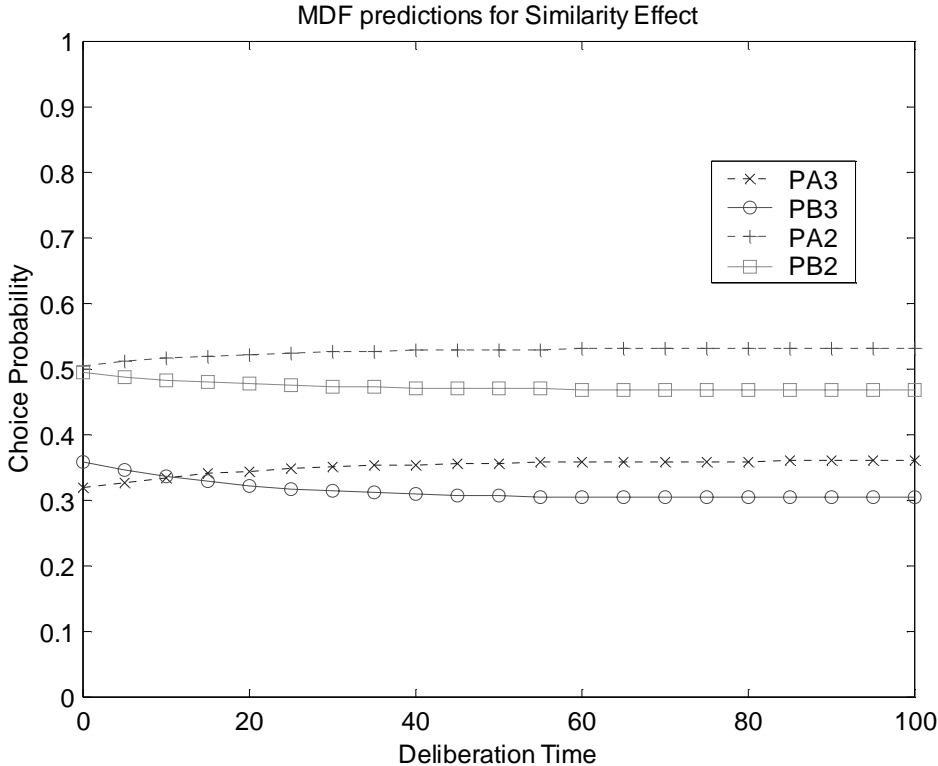


Figure 10

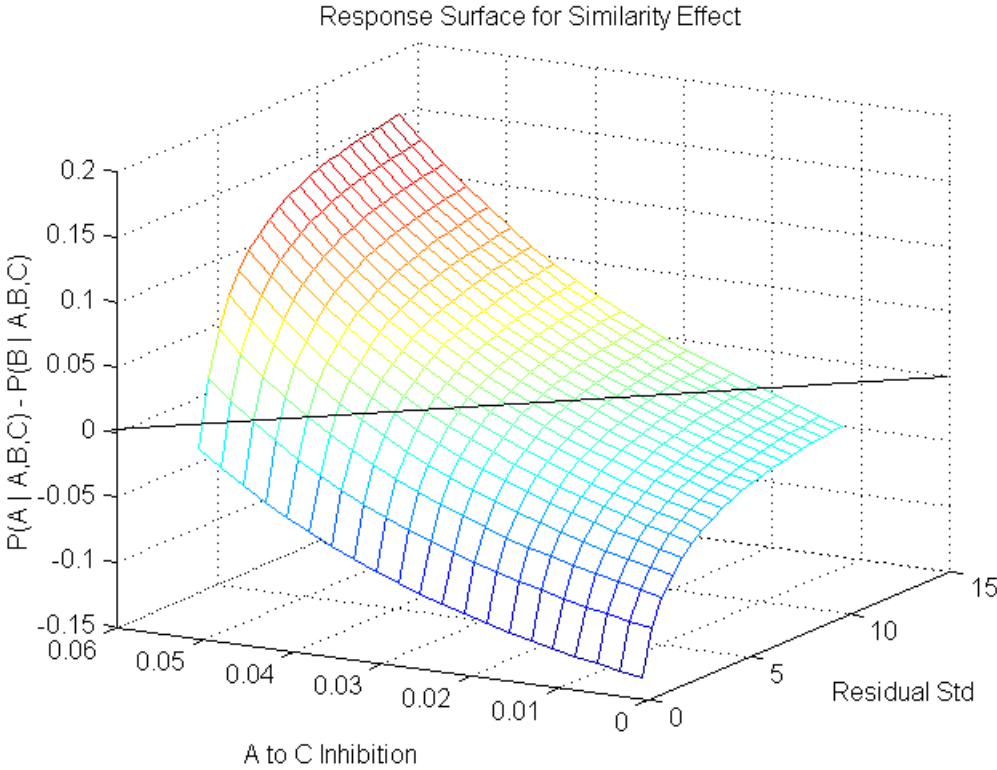


Figure 11

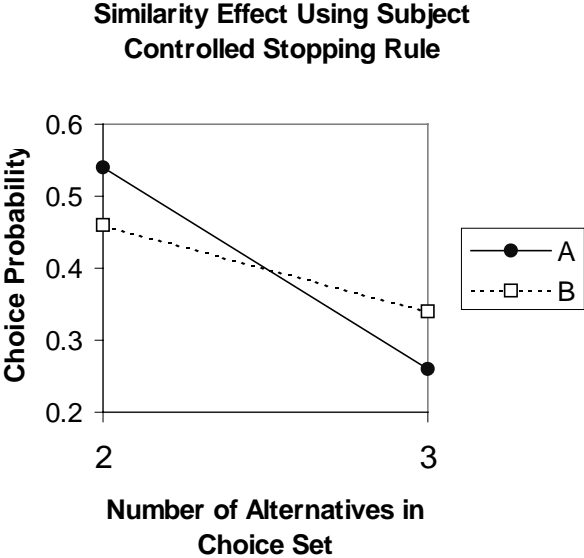


Figure 12

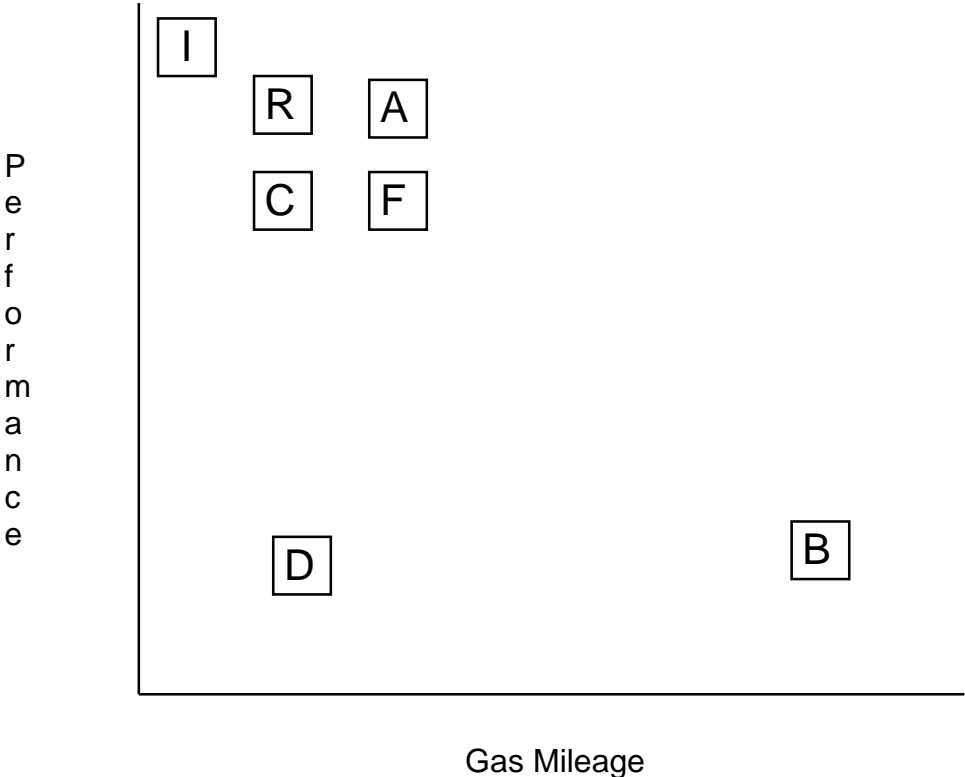


Figure 13

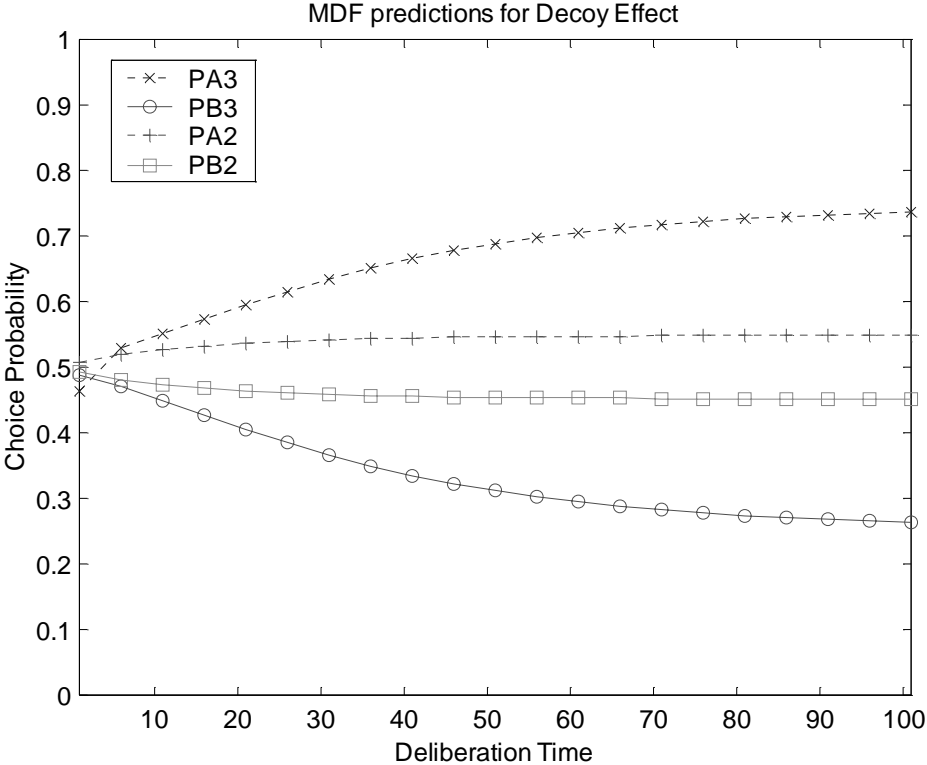


Figure 14

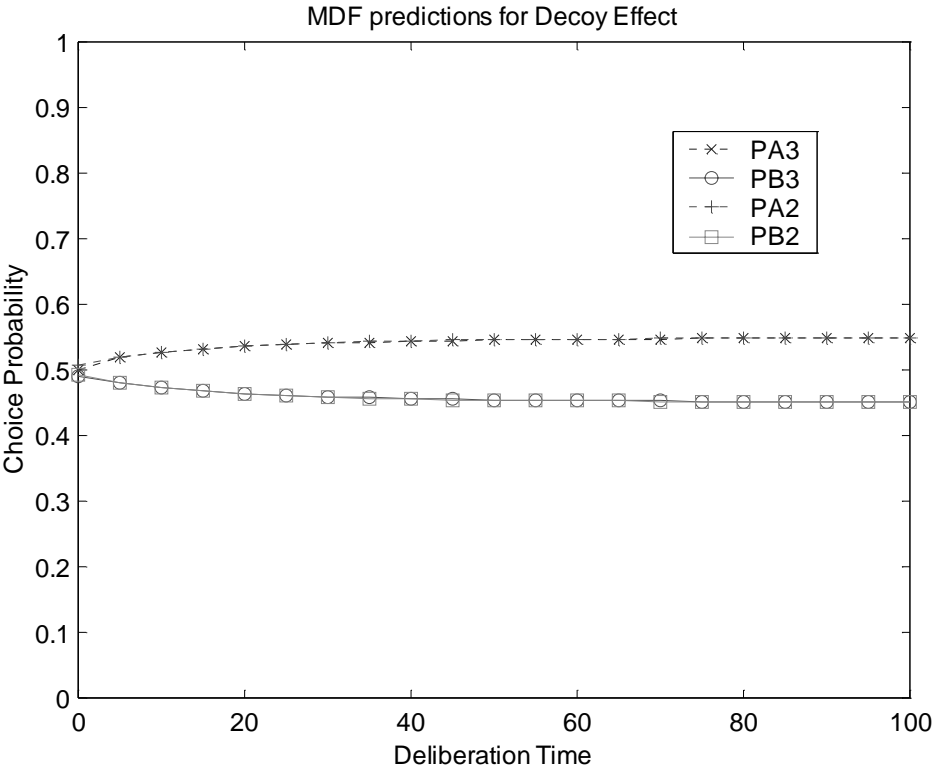


Figure 15

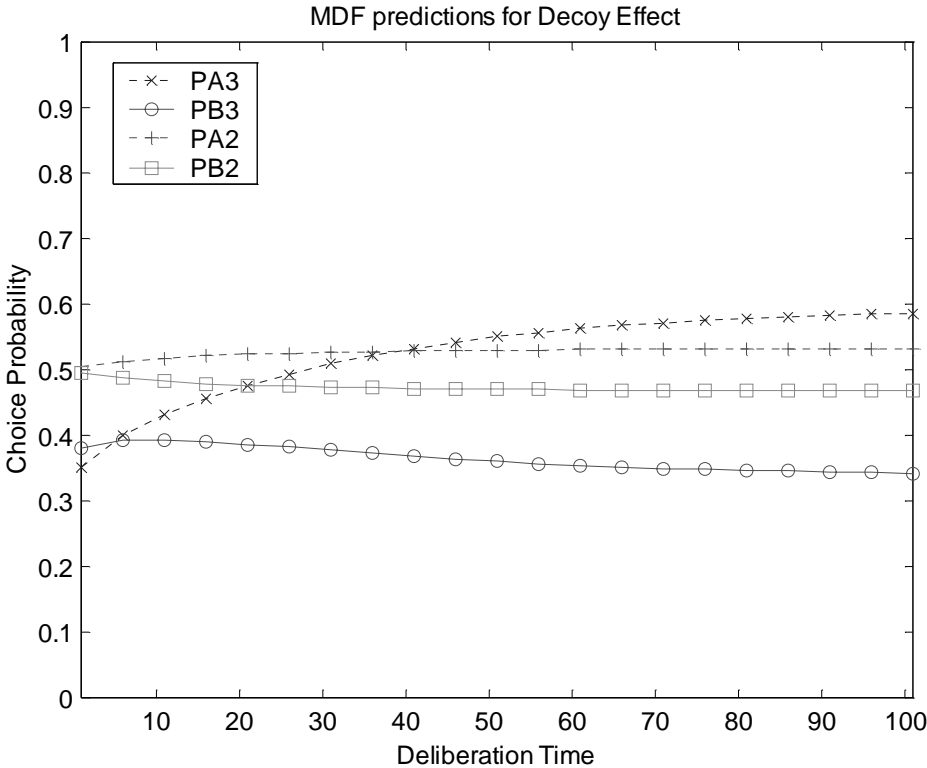


Figure 16

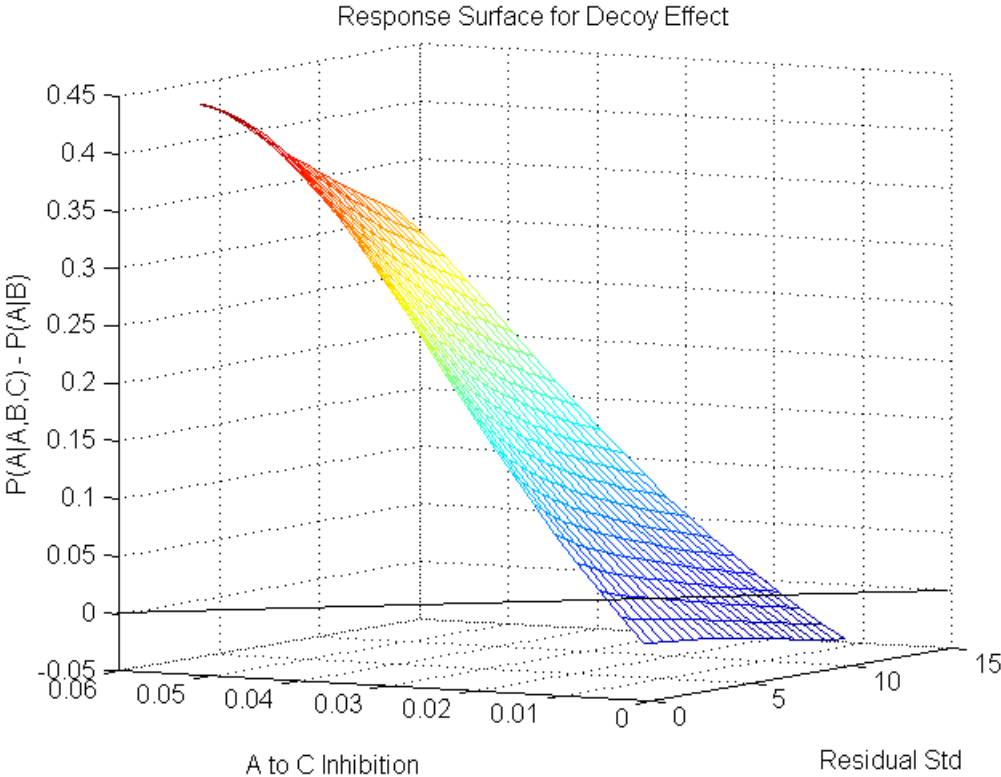


Figure 17

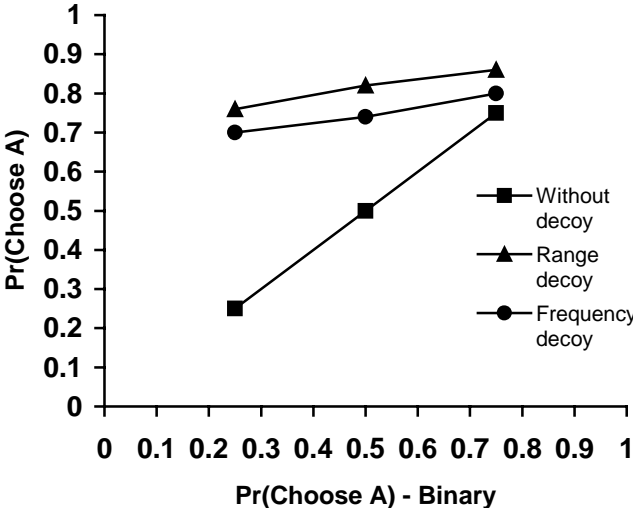


Figure 18

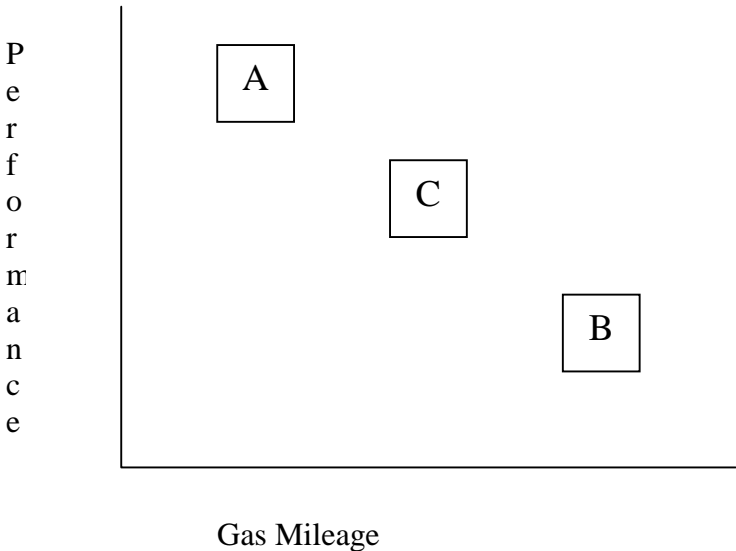


Figure 19

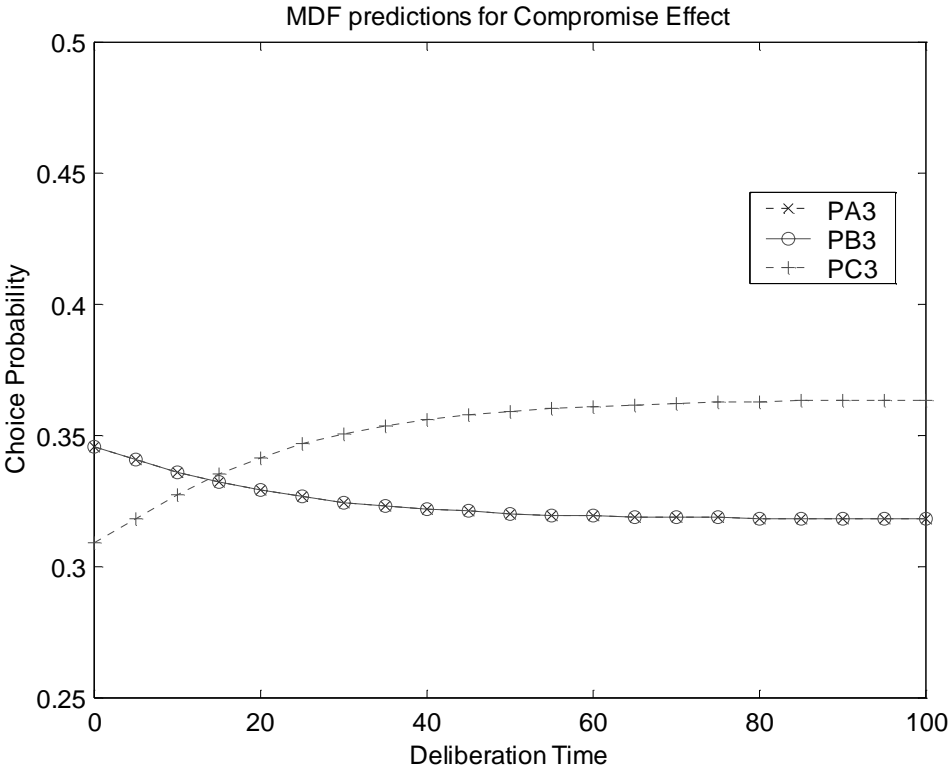


Figure 20

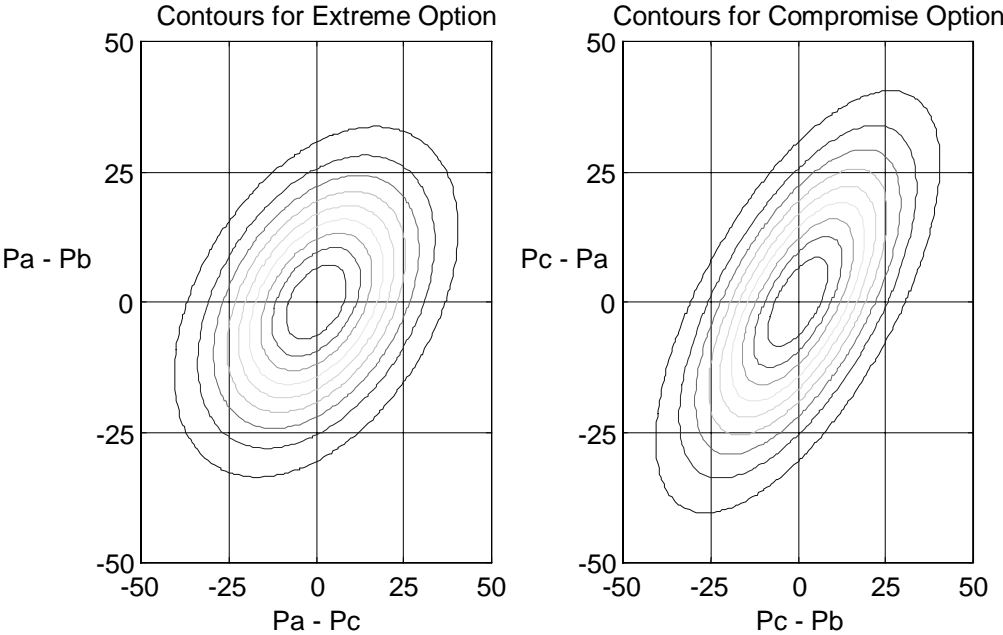


Figure 21

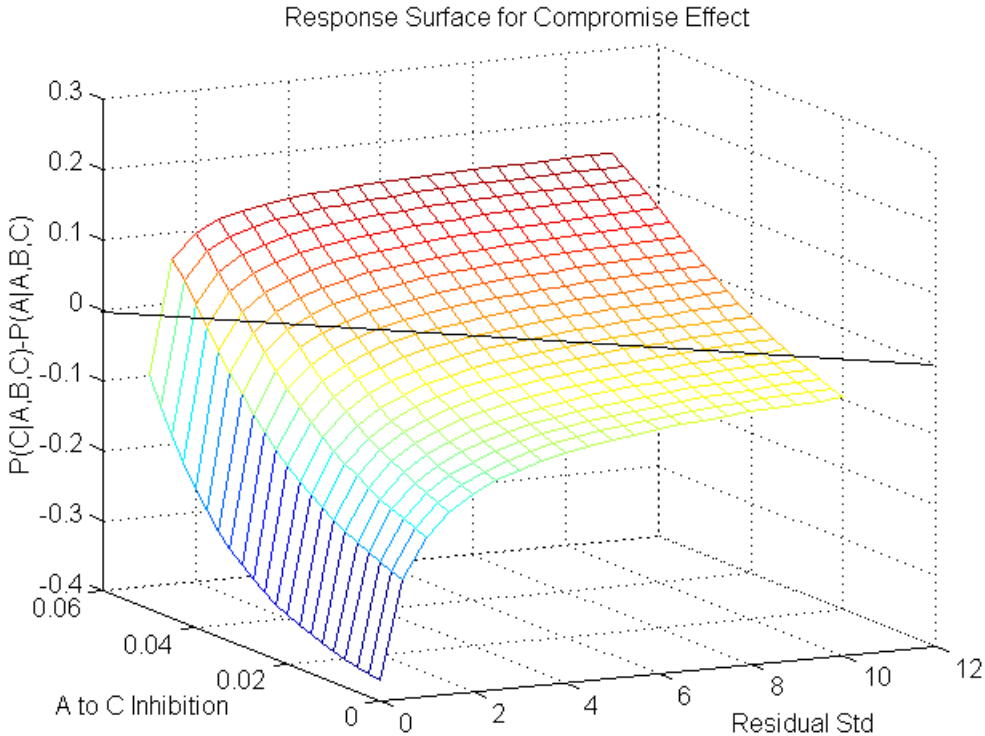


Figure 22

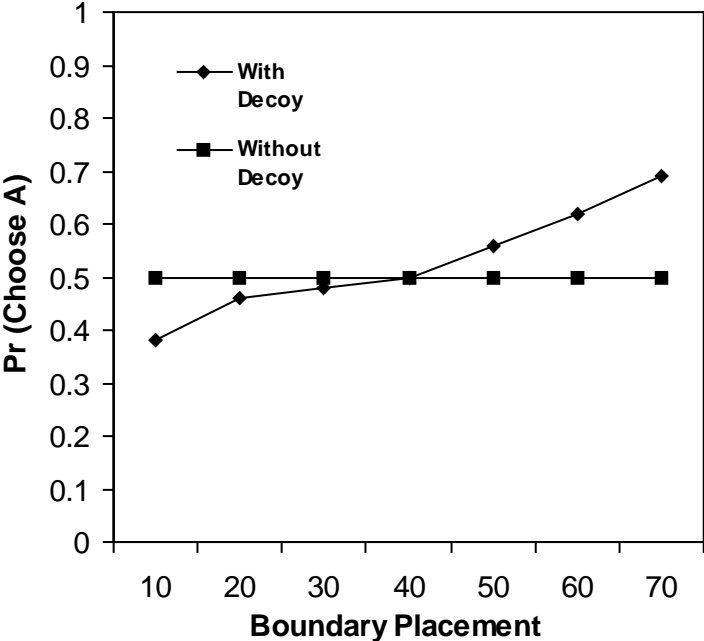


Figure 23

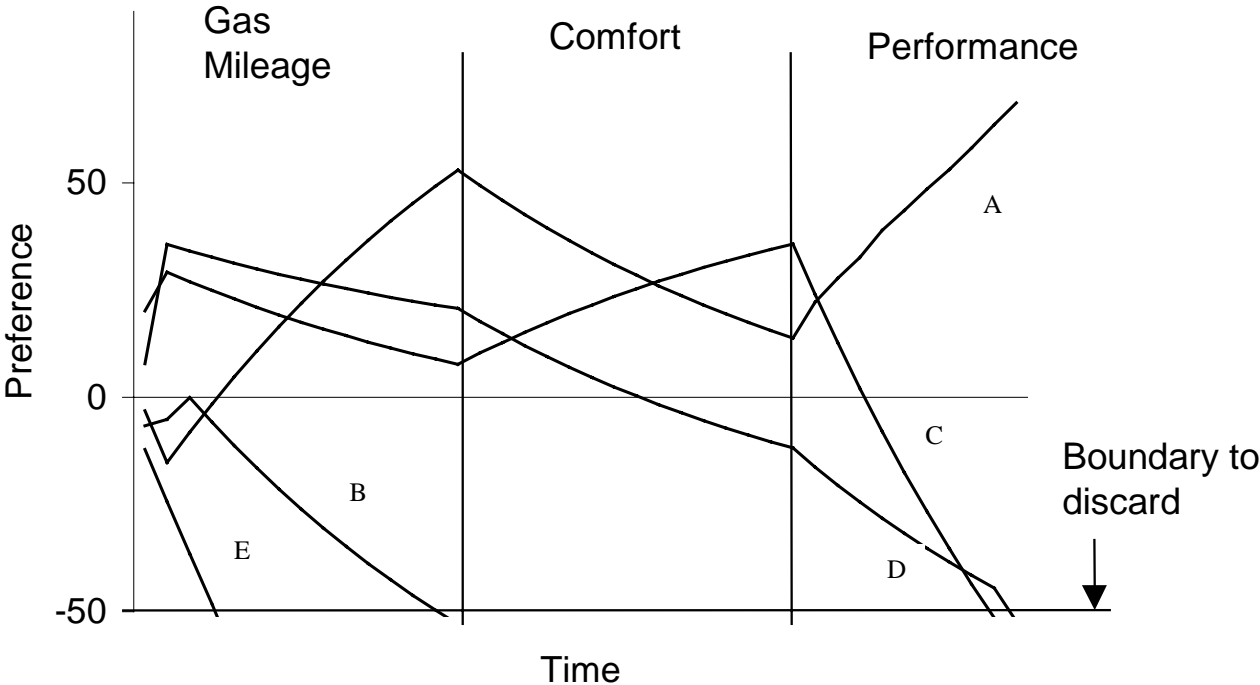


Figure 24

